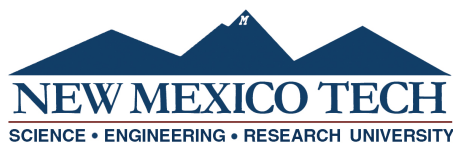


**Estimating The Total Available Water For The Prediction Of Root  
Zone Soil Moisture Using Evapotranspiration and Recharge  
Model**

by

Juliet Ablah Ayertey

Submitted in Partial Fulfillment  
of the Requirements for the Degree of  
Master of Science in Mathematics  
with Specialization in Operations Research and Statistics



New Mexico Institute of Mining and Technology  
Socorro, New Mexico  
August, 2018

## ABSTRACT

The Evapotranspiration and Recharge Model (ETRM) was created to produce accurate estimates of ground water recharge and evapotranspiration for the New Mexico statewide water assessment. The model consistently produced results that deviated significantly from actual observations due to inaccurate Total Available Water (TAW) values used to run the model. This thesis adopts the history matching method to estimate and produce TAW values that fit the actual field observations reasonably better than the TAW values, estimated from soil maps, originally used in the model. This was done by comparing the Root Zone Soil Moisture (RZSM) values from the ETRM output to field measurements of Root Zone Water Fraction (RZWF) collected using the neutron probe from thirteen pixels on the Jornada LTER station located to the north of the Chihuahuan desert in New Mexico. The best fitting TAW values estimated from the history matching method produced significantly smaller chi square values than the original ETRM TAW values in most of the pixels, showing that the TAW values produced in those pixels would produce better estimates of the RZSM when used to run the ETRM. In the other pixels, the chi square values were reasonably close to the original TAW values indicating that the original TAW values were reasonably good values to use in the model. The TAW values were also estimated using remotely sensed observations but the results produced were unreliable because the remote sensing data collected were not extensive (i.e. the observations were very few and most of the values were 0). A sensitivity analysis showed that the annual average recharge estimates obtained from the ETRM, using the best fitting TAW values estimated from the neutron probe observations, were reasonable in terms of magnitude. The analysis also showed the the recharge estimates were significantly underestimated when TAW estimated from remotely-sensed observations were used in the ETRM and overestimated when the original TAW values were used in the ETRM.

**Keywords:** The Evapotranspiration and Recharge Model (ETRM); Total Available Water (TAW) ; Statewide Water Assessment; Root Zone Soil Moisture (RZSM); Root Zone Water Fraction (RZWF); History Matching

## ACKNOWLEDGMENTS

I would like to express my profound gratitude to my academic and research advisor, Dr. Brian Borchers, for his support, guidance, advice and direction throughout my studies and during my thesis work. I would also like to thank Dr. Jan Hendrickx and Dr. Oleg Makhnin for their support as members of my advisory committee. I would also like to acknowledge the support of New Mexico Water Research Institute (NMWRRRI) for the statewide water assessment that generated all the data for this thesis work. I would also like to thank Gabriel Parrish for teaching me almost everything I know about Hydrology and Python. Finally, I would like to show my appreciation to my family and all the faculty, staff and fellow graduate students at the Mathematics department for their support throughout my studies.

This thesis was typeset with  $\text{\LaTeX}^1$  by the author.

---

<sup>1</sup>The  $\text{\LaTeX}$  document preparation system was developed by Leslie Lamport as a special version of Donald Knuth's  $\text{\TeX}$  program for computer typesetting.  $\text{\TeX}$  is a trademark of the American Mathematical Society. The  $\text{\LaTeX}$  macro package for the New Mexico Institute of Mining and Technology thesis format was written by John W. Shipman.

# CONTENTS

<b>LIST OF TABLES</b>	<b>vi</b>
<b>LIST OF FIGURES</b>	<b>vii</b>
<b>LIST OF ABBREVIATIONS</b>	<b>viii</b>
<b>1. INTRODUCTION</b>	<b>1</b>
1.1 Introduction . . . . .	1
1.2 Background . . . . .	1
1.2.1 Description of the Hydrological Cycle . . . . .	2
1.2.2 Total Available Water (TAW) . . . . .	3
1.2.3 TAW Estimates Originally Used in the ETRM . . . . .	5
1.2.4 Root Zone Soil Moisture (RZSM) . . . . .	6
1.3 Problem Statement . . . . .	7
1.4 Objectives . . . . .	7
1.5 Summary of Chapters . . . . .	8
<b>2. LITERATURE REVIEW</b>	<b>9</b>
2.1 Introduction . . . . .	9
2.2 Motivation . . . . .	9
2.3 Compilation of the Work Done in the Other Categories . . . . .	10
2.3.1 Dynamic Statewide Water Budget (DSWB) . . . . .	10
2.3.2 Groundwater Level and Storage Changes . . . . .	10
2.4 Previous Work Done in the Recharge Category . . . . .	11
2.5 Previous Work Done in the Evapotranspiration Category . . . . .	12

<b>3. METHODOLOGY</b>	<b>15</b>
3.1 Introduction . . . . .	15
3.2 Soil Water Balance Model . . . . .	15
3.3 Evapotranspiration and Recharge Model (ETRM) . . . . .	16
3.4 Neutron Probe Soil Moisture Content . . . . .	18
3.4.1 How the Neutron Probe works . . . . .	19
3.4.2 How the Root Zone Soil Water Fraction (RZSWF) is Calculated . . . . .	20
3.5 Remote Sensing of Soil Moisture . . . . .	21
3.6 History Matching . . . . .	22
3.6.1 General Outline For Estimating The TAW Using History Matching . . . . .	23
3.6.2 Justification For Estimating Standard Deviation From The Residuals . . . . .	24
<b>4. FIELD SITE AND DATA</b>	<b>26</b>
4.1 Introduction . . . . .	26
4.2 Project Scope . . . . .	26
4.2.1 Area of Studies . . . . .	26
4.2.2 The Jornada Control Transect . . . . .	29
4.2.3 Data Used . . . . .	29
4.2.4 Analysis of the Pixels . . . . .	30
<b>5. RESULTS AND DISCUSSIONS</b>	<b>33</b>
5.1 Introduction . . . . .	33
5.2 ETRM Run . . . . .	33
5.3 Results and Discussions Using the Neutron Probe Data . . . . .	33
5.3.1 Estimating TAW Using the Neutron Probe Data . . . . .	33
5.3.2 Outliers . . . . .	38
5.3.3 Estimating TAW Using the Remote Sensing Data . . . . .	42
5.3.4 Comparing the Root Zone Moisture Content of the Neutron Probe and Remote Sensing . . . . .	46
5.4 Sensitivity Analysis of the Annual Average Recharge Estimate to the TAW . . . . .	47

<b>6. CONCLUSIONS AND RECOMMENDATIONS</b>	<b>49</b>
6.1 Conclusion . . . . .	49
6.2 Limitations . . . . .	51
6.3 Recommendations . . . . .	51
<b>A. ADDITIONAL INFORMATION ON THE ACCESS TUBES</b>	<b>53</b>
A.1 Minimum and Maximum Storages For Each Access Tube (cm) . . .	53
<b>B. PYTHON CODES</b>	<b>54</b>
B.1 General Python script Used to Find the Best Fitting TAW . . . . .	54
<b>REFERENCES</b>	<b>61</b>

## LIST OF TABLES

1.1	Pixels and Corresponding Estimates of Total Available Water Originally used in the Evapotranspiration and Recharge Model . . . . .	6
4.1	Vegetation Zones and Stations along the Jornada long term ecological research (JRN LTER) Control Transect . . . . .	30
4.2	Depths of Measurement and Representative Layer Thickness . . . . .	30
4.3	Pixels and Access tubes . . . . .	31
5.1	A Table of Optimal Total Available Water (TAW) and 95% Confidence Interval for all 13 Pixels Using Neutron Probe . . . . .	34
5.2	Pixels and Corresponding Total Available Water (TAW) values Originally used in the Evapotranspiration and Recharge Model (ETRM)	37
5.3	Table of Outliers and Corresponding Dates . . . . .	41
5.4	A Table of the best fitting Total Available Water (TAW) for all 13 Pixels Using Remote Sensing . . . . .	42
5.5	Comparing Root Zone Water Fraction (RZWF) Values of Neutron Probe and Remote Sensing . . . . .	47
5.6	Comparing the Annual Average Recharge Rates Between the Estimated and Original Values of the Total Available Water . . . . .	48

## LIST OF FIGURES

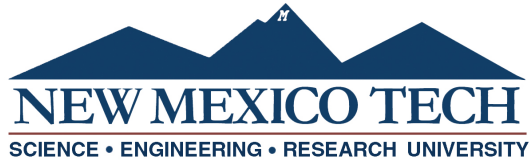
Figure 1.1 The Hydrological Cycle [104] . . . . .	3
Figure 3.1 Structure of a Typical Neutron Probe (Adapted from [12]) . .	19
Figure 4.1 A Map of The Jornada LTER Station (Source: LTER Site profiles [10]) . . . . .	27
Figure 4.2 Locations of the 13 pixels along the Jornada Transect with Neutron Probe Tubes (Source: G. Parrish, Personal Communication, May 08, 2018) . . . . .	31
Figure 5.1 Chi Square Plots For all Thirteen Pixels (Pixels 0 and 1) . . .	34
Figure 5.2 Chi Square Plots For all Thirteen Pixels (Pixels 2 – 7) . . . .	35
Figure 5.3 Chi Square Plots For all Thirteen Pixels (Pixels 8 – 13) . . . .	36
Figure 5.4 The Z-Score Histograms For all Thirteen Pixels (Pixels 0 and 1) . . . . .	38
Figure 5.5 The Z-Score Histograms For all Thirteen Pixels (Pixels 2 – 7)	39
Figure 5.6 The Z-Score Histograms For all Thirteen Pixels (Pixel 8 – 12)	40
Figure 5.7 Remote Sensing: Chi Square Plots For all Thirteen Pixels (Pixels 0 – 3) . . . . .	43
Figure 5.8 Remote Sensing: Chi Square Plots For all Thirteen Pixels (Pixels 4 – 9) . . . . .	44
Figure 5.9 Remote Sensing: Chi Square Plots For all Thirteen Pixels (Pixels 10 – 13) . . . . .	45



## LIST OF ABBREVIATIONS

<i>ALEXI</i>	Atmosphere Land Exchange Inverse
$D_e$	Depletion in the total evaporable water soil layer [mm]
$D_{rew}$	Depletion in the skin layer [mm]
$D_r$	Depletion in the root zone [mm]
$E$	Evaporation [mm/day]
$ET$	Evapotranspiration [mm/day]
<i>ETRM</i>	Evapotranspiration and Recharge Model
$K_{cb}$	Basal Crop Coefficient
$K_e$	Soil Evaporation Coefficient
$K_s$	Stress Coefficient
<i>MLT</i>	Snow melt [mm]
<i>METRIC</i>	Mapping ET at high Resolution and Internalized Calibration
<i>MODIS</i>	Moderate Resolution Imaging Spectroradiometer
<i>NMWRRRI</i>	New Mexico Water Resource Research Institute
<i>NDVI</i>	Normalized Difference Vegetation Index
$P$	Precipitation [mm]
<i>REW</i>	Readily Evaporable Water [mm]
<i>RO</i>	Run Off [mm]
<i>RZSM</i>	Root Zone Soil Moisture
<i>RZSWF</i>	Root Zone Soil Water Fraction
<i>SEBAL</i>	Surface Energy Balance Algorithm for Land

<i>SSEB</i>	Simplified Surface Energy Balance
<i>SWA</i>	Statewide Water Assessment
<i>TAW</i>	Total Available Water [mm]
<i>TEW</i>	Total Evaporable Water [mm]



This thesis is accepted on behalf of the faculty of the Institute by the following committee:

Brian Borchers

---

Academic and Research Advisor

Oleg Makhnin

---

Committee Member

Jan M.H. Hendrickx

---

Committee Member

I release this document to the New Mexico Institute of Mining and Technology.

---

Juliet Ablah Ayertey

Date

# CHAPTER 1

## INTRODUCTION

### 1.1 Introduction

The purpose of this study is to develop a procedure that will estimate the Total Available Water for the prediction of the root zone soil moisture using the Evapotranspiration and Recharge Model (ETRM). This study is part of a larger project whose ultimate goal is to develop a procedure which will provide an economical assessment of evapotranspiration (ET), groundwater recharge, streamflow and crop consumptive use over the entire state of New Mexico (NMWRRRI SWA [17]). These assessments will be part of information needed by the New Mexico Water Resource managers to study and analyze the water budgets for the state of New Mexico. This study focuses on finding ways to make more accurate predictions of the amount of soil moisture in the root zone because accurate estimates of the root zone soil moisture content vastly improves the assessment of evapotranspiration, groundwater recharge and availability of water in the state of New Mexico generally.

### 1.2 Background

In 1963, the New Mexico State University Board of Regents established The New Mexico Water Resources Research Institute (NM WRRRI), the institute was founded with the fundamental purpose of developing and propagating knowledge that will aid in solving problems related to water resources in New Mexico [14]. The institute serves as a center for coordinating research pertaining to water resources across the state. A statewide soil water balance model called the Evapotranspiration and Recharge Model (ETRM), was created to independently assess and obtain estimates of evapotranspiration (ET) and groundwater recharge based on readily available databases with meteorological, land cover and soil information (Ketchum, 2016)[64]. This model was created exclusively for assessment on non-irrigated lands.

The beta version of ETRM was implemented in Python by David Ketchum in 2016 [64]; it showed that the state wide mapping of ET and groundwater recharge can be done in a cost- effective manner using current technology and databases. The ETRM covers the state evenly with over five million  $250m \times 250m$  cells. These cells are known as pixels in this study and each pixel holds values that correspond to physical characteristics of the soil that are consistently unchanging over time such as Total Available Water (TAW), the maximum quantity of water that the soil can hold in its root zone and saturated hydraulic conductivity, the rate at which water infiltrates the soil at the land surface.

Evapotranspiration is a process that describes how soil loses water to the atmosphere through the soil (evaporation) and plants (transpiration) [2]. Transpiration and evaporation happen simultaneously. In places where the crop coverage is small (i.e. vegetation does not fully cover the soil), water is predominantly lost from the soil through soil evaporation, and at places where most of the soil is covered by vegetation, water is primarily lost through transpiration (i.e. loss of water vapor through the pores of leaves). The illustration of the repeated movement of water (which also shows the process of evapotranspiration and groundwater recharge) on the earth surface, underneath the surface of the earth and in the atmosphere is seen in figure 1.1.

### 1.2.1 Description of the Hydrological Cycle

The hydrological cycle, as shown in figure 1.1 is initiated when the heat from the sun allows for water to evaporate from the surface of the oceans, streams and other bodies of water. As the evaporation (process where water changes from liquid to gas [6]) proceeds, the warm moist air rises up and cools down. Condensation (conversion of gas (water vapor) to liquid[6]) occurs and water vapor is transformed to clouds and sometimes, fog or dew. The water falls to the ground as precipitation (rain, snow, etc). When the water hits the ground surface, it is either lost to the atmosphere through ET or it seeps through the soil as groundwater recharge and is stored in groundwater bodies and aquifers. The remainder of the water that stays on the surface of the soil (i.e. the water that is not lost to ET or become groundwater recharge) runs off the surface into the nearest water body and the cycle begins all over again [18].

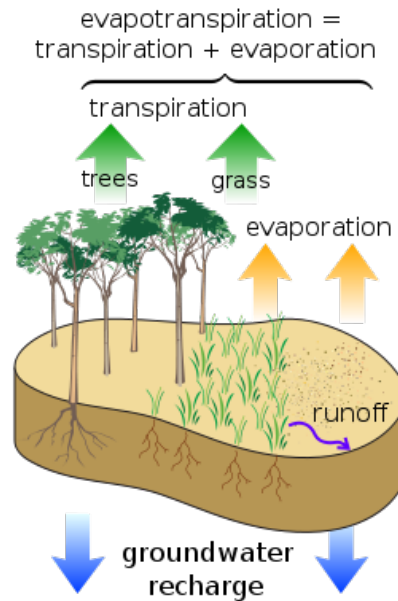


Figure 1.1: The Hydrological Cycle [104]

An important soil factor that has notable effect on the accuracy of the ET estimate with the ETRM is the Total Available Water (TAW).

### 1.2.2 Total Available Water (TAW)

Total Available Water is an important parameter in this model for the assessment of ET, recharge and soil moisture dynamics in ecohydrology (study of interactions between water and the ecosystem). It measures the soil's ability to retain water in the root zone and make it adequately available for plant use (Allen et al,1998[25]). Synonymously, TAW portrays the maximum quantity of water (readily available for crop consumption) that the soil is capable of storing in its root zone. The soil type and the rooting depth of the soil (depth at which plant roots can productively absorb water and nutrients for growth) are the most significant influences on the magnitude of the total available water.

Different terms have been used to describe TAW in different literature such as Water Holding Capacity of Soils (Isrealson and West, 1922; Milly and Dunne, 1994 ) [62][73], Plant Available Water (Kirkham, 2005)[66], Plant-Available Water-Holding Capacity (or simply, storage capacity)(Milly,1994)[73], Available Water Capacity (Cassel and Nielsen, 1986)[40] and extractable soil water capacity (Ladson et al, 2006 [68]). Romano and Santini (2002)[89] called the TAW "the maximum amount of soil water available to plants under field conditions". The term

TAW used in this study is adopted from the FAO Irrigation and Drainage Paper no. 56 (Allen et al,1998[25]). Field capacity is characterized as the measure of water that an all around drained soil can hold against the force of gravity acting on it, or the measure of water remaining when the draining in the soil has fundamentally diminished (Allen et al,1998, P.161) [25]. When no water is supplied to the soil, plants extract the water stored up in the root zone and this causes a reduction in the water in the root zone. As the decrease in the root zone water continues due to extraction, the forces holding the water in the soil become greater. This causes the potential energy to reduce leading to a increase in the difficulty with which the water is extracted by plants. Ultimately, a point is reached where the plant can no longer extract any of the remaining water in the soil. The water uptake goes to zero and wilting point is attained (Allen et al,1998[25]). At this point, plants are no longer able to extract water through their roots in the root zone due to unsuitable conditions and the plants begin to wilt permanently. Since the water content above field capacity drains out because the soil is unable to hold onto the water against the forces of gravity acting on it and the amount of water below wilting point cannot be extracted by the roots of plants, the total available water that is stored in the root zone is then described as the scaled difference between the amount of water in the soil at field capacity and wilting point. The fundamental idea for determining TAW is as follows (Romano and Santini, 2002[89]):

$$TAW = (\theta_{fc} - \theta_{wp})Z_r \quad (1.1)$$

Where:

TAW is the total available soil water in the root zone (*mm*)

$\theta_{fc}$  is the amount of soil water at field capacity ( $m^3/m^3$ )

$\theta_{wp}$  is the amount of water soil water at wilting point ( $m^3/m^3$ )

$Z_r$  is the effective plant rooting depth (*mm*).

Equation (1.1) works under the assumptions that: (i) the amount of soil water at field capacity and wilting point have a constant depth throughout the root zone (ii) the volumetric measure of the soil water at field capacity and wilting point can be derived in the laboratory with a high level of precision and (iii) the effective rooting depth at which plants take up water can be determined from field observations in trenches dug in the soil. These assumptions may hold when dealing with agricultural lands with comparably shallow rooting depths but this equation may fail to work in fields with intricate structures or even in agricultural fields in general (Hendrickx et al, 2016 [58]).

An updated definition of the TAW was determined, which accounts for not only vertical variability of soil texture and structure but also of root distribution and root water uptake (Ladson et al, 2006; Ritchie, 1981a [68][87] ):

$$TAW_{field} = \int_0^{Z_{max}} (\theta_{highest} - \theta_{lowest}) dZ \quad (1.2)$$

Where:

$Z_{max}$  is the maximum depth of the water content measurements

$\theta_{highest}$  is the highest volume of water measured in the field

$\theta_{lowest}$  is the lowest volume of water measured in the field

### 1.2.3 TAW Estimates Originally Used in the ETRM

The TAW used in the ETRM was estimated using soil data viewer (a tool used for creating soil-based maps specific to a particular region [15]) and National Resource Conservation Service (NRCS) databases (Ketchum, 2016 [64]). The databases consist of soil maps (Soil Survey Geographic database (SSURGO) and State Soil Geographic database (STATSGO) (source: web soil survey)[20]). The soil data obtained from the soil maps are used to estimate the amount of soil water at field capacity and amount of soil water at permanent wilting point, which are traditionally used to calculate the TAWs using equation (1.1) and sometimes, these soil data may contain TAW values. From the equation (1.1), another factor of interest needed in estimating the TAW used in the ETRM was the rooting depth, which was estimated from the USGS land cover map (source: USGS land cover site, [19]).

In the calculation of these TAWs, it is assumed that the rooting depth is uniform across a pixel. However, in practice, the rooting depth may not be uniform across a particular pixel. In some areas, there may be no recorded estimate of the rooting depth.

The table below shows the original TAW values used in the ETRM for each pixel (see section 4.2.4) in the study.



Pixel	TAW (mm)
0	257
1	244
2	249
3	220
4	198
5	163
6	163
7	163
8	147
9	157
10	113
11	144
12	144

Table 1.1: Pixels and Corresponding Estimates of Total Available Water Originally used in the Evapotranspiration and Recharge Model

#### 1.2.4 Root Zone Soil Moisture (RZSM)

Soil moisture is defined as the water contained within the spaces that lie between soil particles. The water that is found top layer ( i.e. the upper 5 to 10 centimeters) of the soil is the surface soil moisture while the water that is available and easily accessible by plant roots is the root zone soil moisture, and it can vary from very shallow (10-20 cm) to deep (200 cm or more) depths.

Root zone soil moisture has a significant effects on the rates of evapotranspiration and groundwater recharge, especially in the vegetated regions. Root zone soil water is described in terms of the TAW as the percentage of the TAW that is actually stored in the root zone. The relationship between the root zone soil moisture and the total available water in the ETRM is:

$$RZSM = 1 - \frac{D}{TAW} \quad (1.3)$$

Where RZSM is the root zone soil moisture and D is the depletions (i.e. the water that has left the root zone through evapotranspiration), measured in millimeters. Equation (1.3) forms the basis of the estimation of the TAW for the prediction of the RZSM.

### 1.3 Problem Statement

In order to accurately estimate evapotranspiration and groundwater recharge using the ETRM, it is imperative to accurately predict the amount of soil water in the root zone because the water that is collected in the root zone is subject to evaporation, transpiration and recharge (deep percolation) is found in the root zone. Ketchum's thesis [64] showed that the recharge estimates produced by the ETRM were essentially different from the recharge estimates produced by the chloride Mass Balance (a method that makes use of chloride anions (negatively charged ions) to estimate recharge). Also, the ET values produced by the ETRM differ significantly from the ET values measured in the field by the Eddy covariance method. The Eddy covariance method is a universal, precise and straightforward technique used to measure the variations of energy between the soil surface and the atmosphere (energy fluxes), water vapor, carbon dioxide and other gases [21]. These fluxes can be attained by calculating the covariance of changes in the vertical wind velocity and in the physical quantity of interest (William et al, 2004 [106]).

It is assumed that the error could be a result of the variability in the RZSM which stems from the use of inaccurate TAW values, which were calculated from soil data as discussed in section 1.2.3. The inaccuracies of the TAW could be because the traditional method used calculate the TAW was developed for agricultural lands but does not work very well in deserts, rangelands, riparian areas and mountainous regions. In response to this problem, this study proposes to estimate a trustworthy TAW value on a pixel-by-pixel basis. The aim is to find the optimal TAW value that should be used for each pixel in the area of study. This can be achieved by finding the TAW that minimizes the normalized difference between the root zone soil moisture predicted from the ETRM and the measurements of soil moisture observed from neutron probes and remote sensing in the Jornada for each 250m resolution pixel.

### 1.4 Objectives

In order to achieve the goal of this study, the main objective set for this study is to develop a procedure to estimate the optimal TAW from observations of root zone soil moisture (observed from neutron probe and remote sensing) using the ETRM with 95% confidence interval by using the method of history matching. The optimal TAW in this case is the TAW that produces the minimum chi square value.

## **1.5 Summary of Chapters**

This thesis is made up of six chapters with Chapter 1 being the Introductory chapter and Literature Review making up Chapter 2. Chapter 3 deals with the ETRM model used in the assessment and other methods used to estimate the best fitting TAW and Chapter 4 discusses the area of study and the data used. Chapter 5 constitutes the analysis of the data, statistical outputs and results and discussions and lastly, Chapter 6 is comprised of the conclusion, limitations and recommendations.

## CHAPTER 2

### LITERATURE REVIEW

#### 2.1 Introduction

This chapter reviews the previous works which have been done since 2014 towards the Statewide Water Assessment. This chapter briefly describes the other components of the assessment and then describes into some detail, the work that has been done so far in the ET and Recharge category. This chapter is aimed at providing background knowledge to the intent behind the assessment and the role of this study in the overall goal.

#### 2.2 Motivation

In 2014, the NMWRRRI began a statewide assessment of water resources in the state of New Mexico [14]. This water assessment was aimed at providing advanced, effective and spatially representative evaluations of water budgets to be used in all of New Mexico [17]. These assessments will also be updated frequently and will be easily accessible to the whole state. The projects that are included in the statewide water assessment introduce new technologies that seek to broaden existing studies and can be applied statewide. The water budget components that are very crucial in this assessment are Crop Consumptive Use, Evapotranspiration, Groundwater Recharge and Streamflow. Funds have been provided to the NMWRRRI (FY15, FY 16 and FY 18 funds) by the New Mexico Legislature for this purpose. NMWRRRI uses these funds to coordinate different components of the statewide water assessment which are being researched by various researchers from various institutions across the state such as: New Mexico State University (NMSU), New Mexico Institute of Mining and Technology (NMT), University of New Mexico (UNM), US Geological Survey (USGS), New Mexico Bureau of Geology and Mineral Resources, Petroleum Research Centers, Office of the State Engineer, Sandia National Laboratories and Tetra Tech. The various categories addressed in this assessment are : Dynamic Statewide Water

Budget, Evapotranspiration, Groundwater Level and Storage Recharge, Precipitation, Produced Water, Recharge and Streamflow. This study, however, concentrates on aspects that would improve estimates in the evapotranspiration and recharge category.

## **2.3 Compilation of the Work Done in the Other Categories**

### **2.3.1 Dynamic Statewide Water Budget (DSWB)**

The DSWB seeks to account for the source and future of New Mexico's water resources through time. Two main things that are taken into consideration when accounting for water resources are the area over which the accounting will occur (Spatial Resolution) and the smallest amount of time over which the accounting terms will be averaged (Temporal Resolution). Stocks are used to define the quantity of water a particular category stores in a specific area over a given amount of time and fluxes are used to determine the quantity of water that moves from one stock to another or the entry and exit of water in a given area of interest. The information obtained from the DSWB can aid in local and regional education and planning of water resources to improve the state's control over limited and extremely important water resources. In the first year of the project, Peterson et al (2015) [81] developed a monthly timestep mass balance which accounts for water stocks and flows in New Mexico by major river basins of the state from the year 1975 through 2013. In the second year of the project, Roach et al (2016)[88] concentrated on ensuring there is reasonable consistency between Water Planning Region (WPR) and county level spatial scales. During the project, emphasis was placed on the Middle Rio Grande (MRG) planning region where at a WPR scale, the Middle Rio Grande Conservancy District conveyance infrastructure (water flow in ditches and drains) was internal, but at a county level there was a substantial amount of water entering and leaving counties not through the river, but through conveyance systems.

### **2.3.2 Groundwater Level and Storage Changes**

Groundwater is the water present underneath the soil surface in the soil's pore spaces and in the crevices in rocks. Groundwater is a principal freshwater resource for industrial, agricultural and municipal use in New Mexico. Variations in the groundwater levels is an indication of changes to the total water storage within an aquifer or aquifer system, which can underline the changes in either recharge or discharge. Understanding the changes in the groundwater levels is

also useful in the general evaluation of freshwater resource and its allocation. In the first year of the project, Carroll and Timmons (2015)[107] performed an assessment of spatiotemporal groundwater level changes throughout New Mexico. In their study, they sought to: i) transmit data from a groundwater database into a Geographic Information System (GIS) to map out the spatial distribution of groundwater level variations for visual and spatial analysis, ii) calculate groundwater elevation, change in groundwater elevation, and change in groundwater pumping and population, and iii) evaluate the potential influence of increased groundwater pumping on changes in groundwater elevation. The potential influence was analyzed by comparing the changes in groundwater elevation change and groundwater pumping through space and over time.

In an adjoining project, Rinehart et al (2015)[84] conducted a study on groundwater level and soil changes in various regions of New Mexico. The purpose of the study was to (1) compile water level data from throughout the state, and (2) develop a systematic approach to estimating changes in groundwater storage in alluvial aquifers in the state of New Mexico. In the second year, Rinehart et al (2016)[85] tracked groundwater level and storage changes in basins along the Rio Grande river in New Mexico. In this study, estimates of groundwater storage changes in the alluvial aquifers that occur in the groundwater basins along the Rio Grande were provided to give a more informed insight of the changing water budget in New Mexico. The changes in the groundwater storage for all of the alluvial aquifers in New Mexican Rio Grande basins were estimated by integrating data compilation and review, time series analysis, spatial analysis and interpolation, variations in the volume of water based on the interpolations and aquifer properties.

## **2.4 Previous Work Done in the Recharge Category**

Groundwater recharge, and the ability to quantify it by precipitation, is highly significant in the water assessment and yet, the least understood component in the state water budget. As part of the assessment, Newton, Phillips and Ketchum (2015)[65] sought to compile recharge data and identify recharge areas in the state of New Mexico. The goals of the project in the first year were : (1) to compile existing recharge estimates from different hydrogeologic studies over the last fifty years, and present them in a table and on an interactive map and (2) construct a New Mexico recharge area map within a GIS framework by combining several individual layers containing spatial data that can help determine where groundwater recharge likely takes place. These spatial data sets include a digital elevation model (DEM), precipitation rates, potential ET rates, regional geology, vegetation cover, and soil data. To achieve their goal, a model, written

in the python programming language, was created by the researchers to perform a daily soil water balance for the state. This model, the Evapotranspiration and Recharge Model (ETRM), loads input data (spatial dataset mentioned above) and mathematically models the loss of soil moisture to ET and recharge. The outputs are shown in a format that can be displayed by a GIS.

In the second year of the project, the goal of Newton and Phillips (2016)[84] was to go beyond identifying relative recharge potential to quantifying the recharge. Two significant advances that the researchers sought to make during the second year in order to quantify the recharge were: (1) to upgrade the computational recharge model (ETRM) by considering snow as a water storage, executing a high resolution energy input, and taking modeled runoff into account. Also, the Chloride Mass Balance technique would be used to make independent recharge estimates based on data from the field and (2) to produce independent recharge estimates based on field data. A Chloride Mass Balance (CMB) technique (Ketchum, 2016, P.6)[64] would be used to produce the independent estimates of the recharge. A fact sheet that describes the statewide recharge estimates, the sources of recharge, and estimates of variability was constructed to promote public access to the results of the project. These fact sheets are easily accessible online. They anticipated that the results of the study would provide knowledge of the quantity and location of groundwater recharge, thereby allowing resource managers to make more informed decisions of water use.

## **2.5 Previous Work Done in the Evapotranspiration Category**

Evapotranspiration is an essential component of the statewide water assessment because the ability to accurately model and quantify the temporal and spatial variability of evapotranspiration for a large area is critical in efficiently managing the water resources in the state.

In the first year of the assessment, Samani and Bawazir (2015) [90] proposed using remote sensing technology to improve evapotranspiration estimation. In their work, they established that remote sensing was the most effective way of accounting for ET for large areas. Previous remote sensing models in existence are METRIC (Mapping EvapoTranspiration at high Resolution and Internalized Calibration) (Allen et al, 2007) [29], SEBAL (Surface Energy Balance Algorithm for Land) (Bastiaanssen,1995; Allen et al, 2011) [36] [23], ALEXI (Atmosphere Land Exchange Inverse) (Mecikalski et al, 2002) [72], REEM (Regional Evapotranspiration and Estimation Model) (Samani et al, 2007)[92] and SSEB (Simplified Surface Energy Balance) (Senay et al., 2007, 2011b, 2013, Singh et al., 2014)[99][96][98][102]. Some of these models (e.g. METRIC and SEBAL) use

images from satellites such as MODIS (Moderate Resolution Imaging Spectroradiometer) and Landsat. These models, however, have some limitations such as the inability to capture images in the presence of clouds in MODIS [9]. These limitations sometimes cause discrepancies between the ET estimates produced by the models. REEM, METRIC and SEBAL are time consuming and costly. Part of these problems are mitigated by the METRIC based EEFLUX that provides reasonable ET estimates for flat lands (Foolad et al, 2018)[51] through Google Earth Engine. The SSEB is prone to large errors in contrast to measured and calibrated remote sensing modeled ET values. The goal of their study was to analyze how suitable the SSEB was in the estimation of regional evapotranspiration. In their work, they compared ETs estimated from REEM, SSEB and ALEXI to ground-measured ET using energy budget method by Eddy Covariance Flux Towers. Their results showed that the SSEB model proved promising for regional ET estimation. They then recommended that the SSEB model be further evaluated and modified to estimate regional ET. They believed that this could ultimately become a practical and economical model for large scale estimation of ET and could be used in the water budget for management purposes.

Based on their recommendations at the end of the first year, the goals of Samani and Bawazir (2016)[91] for the second year were to : (1) modify the operational Simplified Surface Energy Balance (SSEBop) model for more accurate estimation of ET in agricultural and riparian vegetation, (2) validate the accuracy of the modified SSEBop model by using results from ground-measured ET and micrometeorological measurements and REEM-generated ET values in New Mexico (Lower Rio Grande and Middle Rio Grande) and (3) organize a workshop to demonstrate the application of the SSEBop model to estimate the evapotranspiration on a regional scale based on Landsat and MODIS images. Landsat captures images of the earth's surface at a 30 meter pixel resolution approximately every fortnight while MODIS captures images at a 250m pixel resolution, which has a wider field of view but a lower spatial resolution (Sesnie et al, 2012 [100]). They used satellite images, which are captured every fortnight, to estimate water use on the land surface. Their method resulted in consistently high resolution ET maps which could be used in various aspects of water budget assessment.

In the same category, Hendrickx, Schmutge and Cadol (2015)[60] performed an analysis on the operational precipitation and evapotranspiration in New Mexico. With precipitation and evapotranspiration being the major components of a water balance equation, they identified five precipitation and three evapotranspiration products currently available in New Mexico. Their goals for the first year were to : (1) compare and contrast the ET and precipitation products on a spatial and statistical level, (2) validate the products against reliable measurements: precipitation products against precipitation gauges and experimental ranges and evapotranspiration against METRIC model ET maps, (3) val-



idate two chosen products for assessment of reference ET which would be used to fill in null values in existing ET products and (4) produce statewide precipitation and evapotranspiration products for New Mexico with a quality assessment and a plan for how to improve these products at the proper spatial and temporal scales. At the end of the first year, they produced spatial maps, graphs, quantitative statistics and histograms for each of the eight models, for the entire state of New Mexico.

In the second year, Hendrickx and Cadol (2016)[59] assessed the soil water balance method for statewide evapotranspiration. Their main goal was to adapt the proven soil water balance method for the estimation of statewide evapotranspiration for groundwater recharge assessment. Their project focused on how ET is affected by topography and quantitative approaches for the calculation of actual ET in challenging topographic environments. In order to achieve their goal, they set four targets : (1) to develop a procedure for calculating reference ET (ET<sub>r</sub>) that includes the effects of slope and aspect of each pixel as well as shadow effects from surrounding pixels, (2) to further develop our procedure to convert ET<sub>r</sub> to actual ET using the operational MODIS NDVI product, (3) to examine the predicted Evapotranspiration estimates in mountainous areas and (4) to prepare a fact sheet, that will be accessible online, to deal with the evaluation of the statewide evapotranspiration from the soil water balance method.

## CHAPTER 3

### METHODOLOGY

#### 3.1 Introduction

This chapter provides insight into the soil water balance model and more specifically, the ETRM model. It talks about the equations and parameters used in the ETRM. This chapter also briefly discusses the procedure used to find the best TAW to use for each pixel.

#### 3.2 Soil Water Balance Model

Ideally, soil water content measurement in the root zone (150 cm and below the earth surface) should be readily available and accessible for every field and vegetation type in the country on a daily basis. This system would provide reliable information on the degree of how dry or wet the soil is. This information would be considerably helpful in the monitoring and management of droughts and floods. However, this kind of system does not currently exist on a large scale. There are presently a number of soil moisture stations (a couple hundreds) all across the United States [16].

Consequently, soil water balance models were created to provide relevant information on soil moisture on a national scale. These models are set to run on a gridded spatial scale. Examples of known soil moisture water balance models are the “Leaky Bucket” model (Huang et al,1996; CPC, 2004 [61] [41]), the North American Land Data Assimilation System (NLDAS) model (Schaake et al, 2004 ; Xia et al, 2014 [93] [108]) and the Vegetation ET (VegET) model (Senay, 2008 [97]).

A classical example of a soil water balance model equation is (Milly, 1994 [73]):

$$\frac{dW}{dt} = P - RO - ET - DP \quad (3.1)$$

Where  $W$  is the volume of water stored in the root zone (mm),  $P$  is precipitation (mm),  $RO$  is surface runoff (mm),  $ET$  is the evapotranspiration (mm) and  $DP$  is deep percolation below the root zone (mm). The equation (3.1) above is a soil water balance equation pertaining to the root zone of a  $30m \times 30m$  resolution Landsat image.

Most soil water balance models make use of precipitation as a primary source of water supply to compute evapotranspiration (which is the water demand element). Other variables instrumental in the process are temperature, solar energy, humidity and wind speed. Soil moisture content, soil temperature and stream runoff are some other parameters that can be estimated from the SWB model. The model is very useful in the estimation of  $ET$  in the arid and semi-arid south-eastern region of the United States. The model makes use of inputs such as rainfall, irrigation water, runoff and snowfall (Ketchum, 2016 [64]).

### 3.3 Evapotranspiration and Recharge Model (ETRM)

The Evapotranspiration and Recharge Model is a soil water balance model that makes use of spatial datasets that supply information about the soil characteristics, topography, geology, vegetation and cover, and climate (precipitation, solar radiation and temperature) to analyze what happens to water from precipitation (rain and snow) after a wetting event in the state of New Mexico. The ETRM uses daily estimates of precipitation, which is provided by the Parameter-Regression and Independent Slopes Model (PRISM) at an  $800m \times 800m$  resolution (Daly et al, 1994 [43] ), as the water supply component to estimate the amount of water that : (i) runs off into streams , (ii) drains into the soil, (iii) is stored within the pores in the soil, (iv) evaporates from the surface of the soil and (v) extracted by plants for use.

The model estimates the  $ET$  by using an adaptation of the FAO-56-Dual Crop Coefficient method (Allen et al, 2005 [27]) and the daily National Land Data Assimilation System reference  $ET$  layer (Lewis et al, 2014 [69]), where the reference  $ET$  uses the alfalfa (tall crop of about 70 cm in height) reference. The FAO-56 (Penman-Monteith) Dual Crop Coefficient method identifies a reference  $ET$  ( $ET_r$ ) value which is used to calculate the actual  $ET$ . By accounting for the moisture in the soil,  $ET_a$  can be evaluated by computing a stress or transpiration reduction coefficient ( $K_s$ ), a basal crop coefficient  $K_{cb}$ , a soil evaporation coefficient ( $K_e$ ) and the reference  $ET$  in a method called the Dual Crop Coefficient Method as shown in equation 3.2 below .

The equation for calculating the actual  $ET$  is:

$$ET_a = (K_s \times K_{cb} + K_e)ET_r \quad (3.2)$$

The basal crop coefficient  $K_{cb}$  is estimated by using NDVI (Normalized Difference for Vegetation Index) gotten from the Moderate Resolution Imaging Spectroradiometer (MODIS). MODIS is a scientific equipment that was constructed by Santa Barbara Remote Sensing and was launched into the earth's orbit by the National Aeronautics and space Administration (NASA) in the years 1999 and 2002.

NDVI is used to evaluate remote sensing estimates and establish whether an area of interest contains live green vegetation or not. Simply put, it is the measure of the greenness of a vegetation. The NDVI is computed for every 16 day period of the year by using the data obtained from the MODIS satellites. The NDVIs are obtained on a day-to-day basis by using a linearly interpolated data set which is weighted between two consecutive 16 day periods. The  $K_{cb}$  is estimated as [56]:

$$K_{cb} \approx 1.25 \times NDVI \quad (3.3)$$

The soil water balance of the root zone on a particular day  $i$ , employed by the ETRM, is (Allen, 2011)[24] :

$$D_{r_i} = D_{r_{i-1}} - (P_i - RO_i) - I_i - CR_i + ET_{ci} + DP_i \quad (3.4)$$

Where where  $D_{r_i}$  and  $D_{r_{i-1}}$  represents the depletions in the root zone at the end of the current and previous day respectively,  $P_i$  is precipitation,  $RO_i$  represents the surface runoff,  $I_i$  is the irrigation depth that infiltrates the soil,  $CR_i$  is the capillary rise from the groundwater table,  $ET_{ci}$  is evapotranspiration and  $DP_i$  is the water drained out of the root zone.

All the depletions that occur in the soil have a minimum value of 0 but there is an added limitation on the depletion in the root zone i.e.

$$0 \leq D_{r_i} \leq TAW \quad (3.5)$$

The stress coefficient ( $K_s$ ) for a particular day  $i$  is calculated as:

$$K_{s,i} = \frac{TAW - D_{r,i-1}}{TAW - RAW} = \frac{TAW - D_{r,i-1}}{(1-p)TAW} \quad \text{for } D_{r,i-1} > RAW \quad (3.6)$$

RAW is the portion of TAW that a plant can readily extract from the root

zone without without being subjected to water stress. Mathematically,

$$RAW = pTAW \quad (3.7)$$

where  $p$  is the portion of the TAW that can be drained before water stress and ET reduction sets in.

The soil evaporation coefficient  $K_e$  depicts the most of the evaporation from the soil after a wetting event facilitated by precipitation or irrigation.

The dual crop coefficient employed an adjusted version of the skin layer evaporation technique (Allen, 2011)[24]. Although this consequently adds some noise to the thickness of the skin layer and the quantity of water that can be accumulated in it, it has the advantage of modeling the evaporation that takes place immediately after a minor wetting event, which is constrained solely by the energy available.

### 3.4 Neutron Probe Soil Moisture Content

The neutron probe, which is also known as the neutron moisture meter, is a nuclear-based piece of equipment that measures the amount of water in the soil (Bacchi et al, 2002 [32]). The neutron probe is a complex equipment that contains radioactive sources which may present health and environmental hazards if not handled (i.e. usage, storage and disposal) properly. It requires calibration and operation by a licensed operator and individual calibrations are made for each soil type or field for more accuracy in the readings. A typical neutron probe consists of a gauge (which consists of the display and a protective shielding made of lead to absorb gamma radiations), a connecting cable and a probe which holds the radioactive materials and a detector (Evet, 2008 [49]).

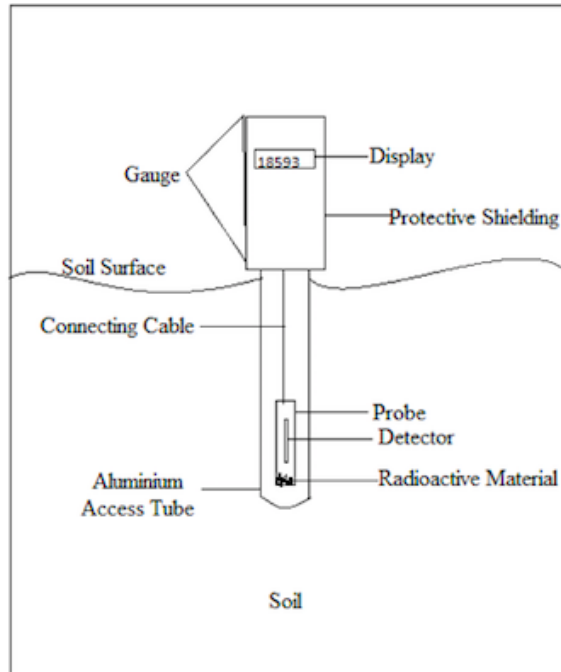


Figure 3.1: Structure of a Typical Neutron Probe (Adapted from [12])

### 3.4.1 How the Neutron Probe works

To install a neutron probe in the soil, a thin-walled access tube is first implanted in the soil through an access hole and the probe is lowered into the soil through it to the depth chosen for measurement. The ideal material for the access tube is aluminium because it is virtually transparent to neutrons and is able to resist corrosion. A typical neutron probe contains a pellet of americium-241 (a radioactive material) and beryllium. As the americium decays, it emits alpha particles which collide with the beryllium. A beryllium atom contains a loosely held neutron in its nucleus. When these nuclei collide with the alpha particles, there is a discharge of a high-energy neutron. These neutrons travel at a speed of 6000 miles per second on average and are therefore called fast neutrons. The fast neutrons are discharged in every direction where a collision occurs with atoms in the soil. The average energy in the collision of the fast neutrons with another atom is considerably greater when the atoms have low atomic mass than atoms with higher atomic mass. Among all the elements that are present in large amounts in the soil, Hydrogen is the only one that has a low atomic weight. Therefore, the fast neutrons mostly collide with the hydrogen atoms in the soil. These collisions cause the neutrons to scatter and lose most of their energy. The neutrons slow down to an average speed of 1.7 miles per second and therefore are called slow neutrons. The slow neutrons are bounced back to the access tube and form a

cloud around the probe. The slow neutrons are counted by a neutron detector. The detection of the slow neutrons returning to the probe makes it possible to estimate the amount of hydrogen present. The hydrogen found in soils is almost entirely in the form of water. Since water contains two atoms of hydrogen per molecule, this subsequently, evaluates the amount of water present in the soil [13].

An advantage of the neutron probe is that it is highly sensitive to variations in the moisture levels of the soil. It also gives more accurate readings of the soil moisture content and readings can be made at different depths within a short period of time. A disadvantage is that soil moisture readings at shallower depths may be unreliable because some the neutrons are lost to atmosphere and are not detected by the probe.

### 3.4.2 How the Root Zone Soil Water Fraction (RZSWF) is Calculated

The counts of the slow neutrons are transmitted to the gauge. The gauge contains a microprocessor with a calibration equation specific to the particular field type being studied. The equation produces a reading of the volumetric quantity of soil water. The soil water is evaluated at different depths, specially determined by the researcher, at each station. The measurement of the thickness of the representative layer of each depth is also recorded. Below are the steps generally followed to calculate the RZSWF;

1. The amount of water stored ( $S$ ), at a particular station is calculated by taking the sum of the product of the volumetric amount soil water at each depth and the corresponding thickness of the representative layer of that depth.
2. Minimum amount of water stored ( $S_{min}$ ) and maximum amount of water stored ( $S_{max}$ ) are recorded by studying the neutron probe readings that were recorded over time (See Appendix A.1). During times when the soil is still actively draining water from the soil after a heavy downpour of rain, the next highest storage value is used as the maximum storage (Source: Hendrickx, J, Personal Communication, June 23, 2018).
3. The storage,  $S$ , is then normalized to get the RZSWF:

$$RZSWF = \begin{cases} \frac{S - S_{min}}{S_{max} - S_{min}}, & \text{if } S_{min} < S < S_{max} \\ 0, & \text{otherwise} \end{cases} \quad (3.8)$$

### 3.5 Remote Sensing of Soil Moisture

Over the years, a variety of remote sensing techniques have been utilized to estimate soil moisture content. Most of these techniques developed ( such as the remote sensing microwave technique (Engman et al, 1995 [48]) and airborne passive radiometers ( Schmugge et al, 1998 [94])) are only able to estimate the amount of soil water in the first few centimeters of the soil. Scott et al, 2003 [95] used remotely sensed optical imagery to map the root zone soil water. They did this by estimating a mathematical relationship between the evaporative fraction (ratio of the latent heat flux to the sum of the latent and sensible heat fluxes) and volumetric soil moisture. The two are related through a standard regression curve that does not rely on the soil type or the vegetation type. The relationship derived by Scott et al was:

$$S = \frac{\theta}{\theta_{sat}} = \exp \left\{ \frac{(\Lambda - 1)}{0.421} \right\} \quad (3.10)$$

given that

$$\Lambda = \frac{\lambda E}{(\lambda E + H)} \quad (3.11)$$

Where:

$S$  is the relative soil moisture

$\theta$  is the volumetric amount of water in the soil

$\theta_{sat}$  is the volumetric amount of water at saturation

$\lambda E$  is the latent heat flux (an energy component of SEBAL)

$H$  is the sensible heat flux to the air (an energy component of SEBAL).

Equation (3.14) was derived using on-site soil moisture measurements from Kansas (alluvial soil and loess, Smith et al, 1992 [103]) and Spain (loamy soil, Bolle et al, 1993 [38]) and was validated using soil water data from irrigated lands in Mexico and Pakistan.

In 2005, Fleming et al [50] adopted equation (3.1) to map root zone soil moisture in the Middle Rio Grande Valley and Sevilleta Long Term Ecological Research (SEV LTER) site. In their research, they concluded that the equation might not work very well on a regional scale in New Mexico because of the wide range of soil types in New Mexico while the Scott's study was conducted on a limited soil types. A root zone water fraction (RZWF) is then defined as:

$$RZWF = \frac{\theta - \theta_{wp}}{\theta_{fc} - \theta_{wp}} \quad (3.12)$$



where  $\theta$  is the volumetric amount of soil water,  $\theta_{wp}$  is the volumetric amount of water at wilting point and  $\theta_{fc}$  is the volumetric amount of water at field capacity.

A stress function proposed by Anderson et al (2007) [30] when they proposed a normalized logistic function that was not dependent on soil characteristics is:

$$\frac{ET}{PET} = \frac{\ln(W)}{\ln(W_f)} \quad (3.13)$$

Where

$$W = \frac{W_0 W_f}{W_0 + (W_f - W_0) \exp(-\mu \times RZWF)} \quad (3.14)$$

Where:

$$W_0 = 1$$

$$W_f = 800$$

$$\mu = 12$$

ET is the actual ET

PET is the Potential ET, whose estimate is established on the Priestly-Taylor Approximation (Priestley and Taylor, 1972 [82])

Using equations (3.13) and (3.14), the RZWF is algebraically estimated as

$$RZWF = -\frac{1}{\mu} \ln \left[ \frac{W_0 \left( e^{-\frac{ET}{PET}} - 1 \right)}{W_f - W_0} \right] \quad (3.15)$$

### 3.6 History Matching

In reservoir modeling, history matching is defined as the method of adjusting a reservoir model until it closely reproduces previous behavior of the model (Schlumberger Oilfield Glossary [4]). A history matched model can be used to simulate future reservoir behavior to a reasonably high confidence level. The accuracy of the history matching method usually depends on the model being used and the quality, as well the quantity of the observed data.

In this study, the concept of history matching was adopted to estimate an input parameter (TAW), based on the historically observed root zone soil moisture values collected from the field (Neutron probe and remote sensing) using the ETRM. The general Procedure followed for the history matching in this study is outlined in the next section below.

### 3.6.1 General Outline For Estimating The TAW Using History Matching

For a particular pixel, the best TAW was estimated from the observed data and the ETRM using history matching using the following steps:

1. Run the ETRM for the simulation (historical) period for different values of TAW.
2. For each day, estimate the residuals ( $r$ ) i.e. difference between the observed root zone water fraction (RZWF) and the modeled RZSM:

$$r = RZWF - RZSM \quad (3.16)$$

3. Calculate the residual sum of squares (RSS):

$$RSS = \sum_{i=1}^m r_i^2 \quad (3.17)$$

The RSS measures the dissimilarity between the measured RZWF and the modeled RZSM (from the ETRM). A smaller RSS indicates a tighter fit of the model to the observed data. The TAW with the smallest RSS is estimated to be the best fitting TAW for that particular pixel.

4. The uncertainties in the field measurements (i.e. standard deviation of the measurement) are not known a priori. Therefore, an assumption is made so that the measurement errors are independent and normally distributed with mean zero and standard deviation  $\sigma$ , where  $\sigma$  can be estimated from the residuals as (Aster et al, 2011, p.38; p.225 [31]):

$$s = \frac{\|r\|_2}{\sqrt{\nu}} \quad (3.18)$$

where  $\|r\|_2$  is the  $\ell_2$ -norm or the euclidean norm of the residuals, i.e.

$$\|r\|_2 = \sqrt{\sum_{i=1}^m r_i^2} \quad (3.19)$$

and  $\nu$  is the number of degrees of freedom and

$$\nu = m - n \quad (3.20)$$

where:

$m$  is the number of days for which the data was collected and

$n$  is the number of parameters.

For this study, TAW is the only parameter being considered ( $n = 1$ ).

$s$  can be rewritten as

$$s = \sqrt{\frac{\sum_{i=1}^m r_i^2}{m-1}} \quad (3.21)$$

5. Using  $s$  calculated from the best TAW estimated from step 3, the chi square statistic is calculated for each TAW as:

$$\chi^2 = \sum_{i=1}^m \left( \frac{RZWF[i] - RZSM[i]}{s} \right)^2 \quad (3.22)$$

Chi square can be rewritten as:

$$\chi^2 = \frac{1}{s^2} \sum_{i=1}^m (RZWF[i] - RZSM[i])^2 \quad (3.23)$$

6. An approximate 95% confidence region for the best TAW is estimated using the inequality

$$\chi^2(TAW) - \chi^2(TAW^*) \leq \Delta^2 \quad (3.24)$$

where:

$\chi^2(TAW)$  is the chi square value at each TAW

$\chi^2(TAW^*)$  is the chi square value at the best fitting TAW

$\Delta^2$  is the 95th percentile of a chi square distribution with  $n$  degrees of freedom.

### 3.6.2 Justification For Estimating Standard Deviation From The Residuals

Both the neutron probe data and the remote sensing data do not have an objective basis for the uncertainty placed on the root zone moisture content values.

In the neutron probe data, however, there was a potential of calculating the uncertainties based on the fact that each pixel had at least two neutron probes collecting data and the resulting RZWF value used for a pixel was the mean RZWF

value for all the neutron probes in that particular pixel. The standard error of the mean was calculated for every pixel and used to find the chi square values and to conduct a chi square goodness of fit test using:

$$\chi^2 = \sum_{i=1}^m \left( \frac{RZWF[i] - RZSM[i]}{se[i]} \right)^2 \quad (3.25)$$

where  $se$  is the standard error of the mean.

This method did not work as expected because the access tubes were not randomly distributed across a particular pixel (all the tubes follow a line that goes through the pixel). Consequently, this led to extremely small estimates of the standard errors and an overestimation of the TAW values. It also failed the chi square goodness of fit test consistently.

The standard deviation,  $s$ , estimated in equation (3.23) comes at a cost where better estimates of  $s$  are estimated with larger sample sizes. A chi square goodness of fit test is unnecessary because a chi square calculated with  $s$  will always pass the chi square test because when equation (3.21) is inserted into equation (3.22),

$$\chi^2 = \sum_{i=1}^m \left( \frac{r_i}{\sqrt{\frac{\sum_{i=1}^m r_i^2}{m-n}}} \right)^2 \quad (3.26)$$

$$= m - n \quad (3.27)$$

$$= \nu \quad (3.28)$$

Thus the chi square value always passes the chi square test (Aster et al, 2011, p.39 [31]).

## CHAPTER 4

### FIELD SITE AND DATA

#### 4.1 Introduction

This chapter looks at the area of interest and data collected for the study. Throughout this chapter, the Jornada Long Term Ecological Research (JRN LTER) station, which is situated in the Chihuahuan Desert, is discussed. This chapter also looks at the stations where the neutron probe and remote sensing data are collected and how they are collected. The pixels considered in this study are also briefly described in this chapter.

#### 4.2 Project Scope

##### 4.2.1 Area of Studies

The area considered for this study was the Jornada Long Term Ecological Research Station (LTER), which is found within the New Mexico State University's Chihuahuan Desert Rangeland Research Center (CDRRC) and the adjoining fields of the USDA Jornada Experimental Range. The Jornada LTER station was established in 1982 to investigate the important factors and procedures that affect the ecosystem dynamics and systems in the Chihuahuan Desert. The station covers approximately 104,166 hectares of land. These landscapes are illustrative of several arid and semi-arid lands in the world where substantial variations in the structures and ecosystems of various vegetations have occurred over some time [7]. The LTER station constitutes approximately 25,900 hectares of the CDRRC land and approximately 78,266 hectares of the USDA land [8] (Anderson and Greenland, 2018 [55]). They are found at the north-eastern part of the Chihuahuan desert, which is to the northeastern side of Las Cruces (approximately 25 km), New Mexico, USA (+32.6°N, -106.7°W, elevation 1188 m). The desert extends from the southcentral part of New Mexico, USA to Zacatecas, a state in Mexico as seen in figure 4.1 below. According to MacMahon et al.(1985) [70], the Chihuahuan desert constitutes about 36% of North American Desert land.

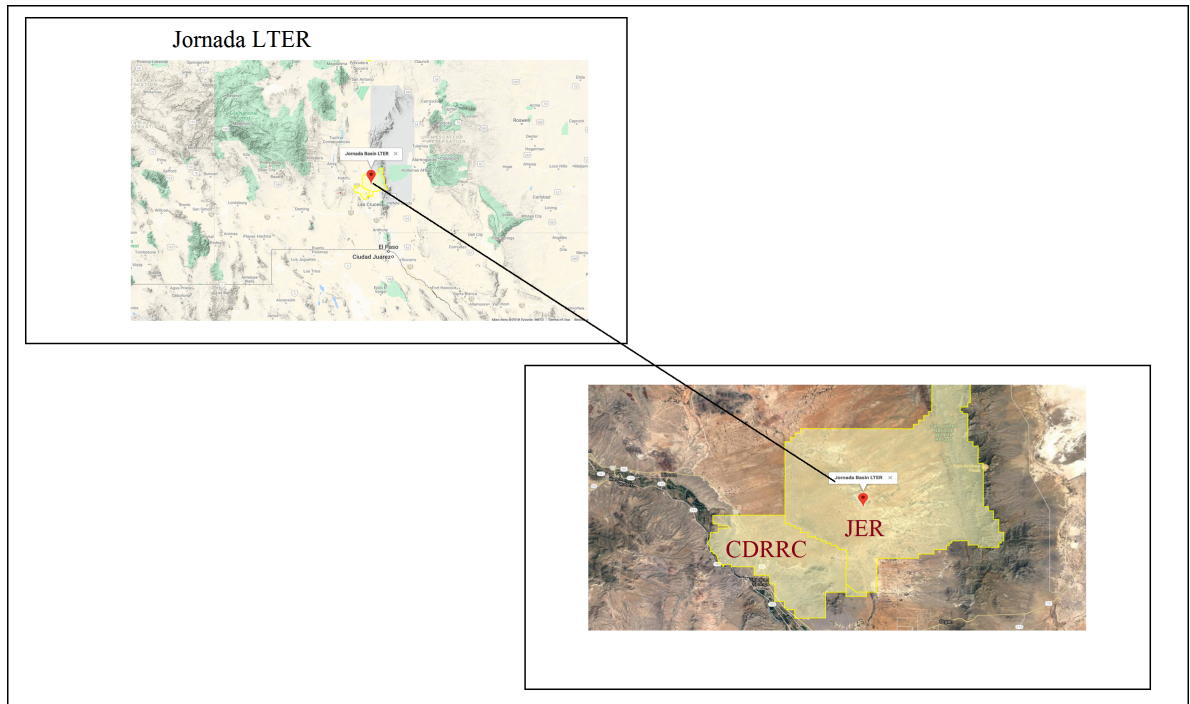


Figure 4.1: A Map of The Jornada LTER Station (Source: LTER Site profiles [10])

The northern Chihuahuan desert has a climate that is marked by high levels of solar radiation. During the day, the desert experiences a wide range of temperatures. It is also marked with low relative humidity and very irregular precipitation patterns. The climate and nature of the deserts consequently leads to potentially high rates of ET. The mean maximum temperature is typically  $36^{\circ}\text{C}$  and this is usually recorded in June. The month of January records an average maximum temperature of  $13^{\circ}\text{C}$ . The annual average precipitation recorded in the desert is 23 cm. 52% of the time, precipitation occurs in the form of transient and confined but severe thunder showers. It usually occurs between the months of July and September (Anderson and Greenland, 2018 [55]).

The Jornada LTER is mainly made up of five vegetation habitats (two grasslands and three shrublands) and records an average temperature of  $24^{\circ}\text{C}$  (McKenna and Sala, 2018) [71]. These can be classified into two main vegetation ecosystems:

1. Grasslands
  - Black Grama Grassland ( *Bouteloua eriopoda* )
  - The Playa Grasslands
2. Shrublands

- Creosotebush Shrubland ( *Larrea tridentata* )
- Mesquite Shrubland ( *Prosopis glandulosa* )
- Tarbush Shrubland ( *Flourensia cernua* )

The Black Grama grasslands are mostly sandy sites filled with deep loam. The soils are rich in calcium carbonate ( $CaCO_3$ ) and have a relatively higher moisture content. The black grama ( *Bouteloua eriopoda* ) is a warm season perennial grass, indigenous to the south-western part of the United States, which usually grows from 0.25 to 0.9 meters. The grass grows well when it is planted in a soil whose temperature is approximately  $10^{\circ}C$  and the ideal time for planting the Black Grama grass is late July to early August. The Black Grama is highly tolerant to drought and it is very instrumental in the prevention of soil erosion (Garner, 2002)[53].

The playas are filled with various grasses including the Tobosa grass (*Pleuraphis mutica*), the Burro grass (*Scleropogon brevifolius*), the Vine-mesquite grass (*Panicum obtusum*) and the Alkali Sacaton grass (*Sporobolus airoides*). They are usually found in low-lying areas that are occasionally flooded with run on water from surrounding areas with higher elevation. The soil types in the playa grassland are usually clay soils (Anderson and Greenland, 2018; McKenna and Sala, 2018) [71] [55].

The creosotebush shrub can grow in a vast variety of locations and soil types. Under the proper conditions, the creosotebush has the ability to adapt and compete with many other plants in its ecosystem. The creosotebush shrubs are known for their longevity (their life span range from hundreds of years to thousands of years) [1].

The honey mesquite is a deciduous shrub that is usually small (usually between 6.1 m and 9.1 m) to medium-sized (usually around 15 m) and has deep roots. Its flowers blossom during the spring and the summer (usually from March to November). These flowers are yellowish, spiky and elongated. The flowers produce yellow seedpods which are rich in proteins and fibres and serve as food source for a variety of animals (such as deer, coyotes, etc), livestock and humans [5].

The tarbush shrubs are deciduous in the winter in most regions are capable of retaining their leaves in areas where there is sufficient moisture. In addition, tarbush is most commonly associated with creosotebush through dominance, co-dominance or sub-dominance [3].

#### 4.2.2 The Jornada Control Transect

The Jornada control transect is a 2.73km transect situated on the New Mexico State University college ranch. Based on the texture, vegetation, morphology and amount of soil water, The transect is classified into seven zones (Nash et al, 1991[76]). The zones are:

1. Playa – Vine Mesquite grassland (*Panicum obtusum*)
2. Playa fringe – Honey Mesquite shrubland (*Prosopis glandulosa*)
3. Basin slope – Soaptree Yucca grassland (*Yucca elata*)
4. Bajada slopes – Creosotebush shrubland (*Larrea tridentata*)
5. Lower piedmont slope – Fluffgrass grassland (*Erioneuron pulchellum*)
6. Upper piedmont slope – Black grama grassland (*Bouteloua eriopoda*)
7. Rocky slope – Turpentine bush shrubland (*Ericamera laricifolia*)

The transect increases in elevation from playa to mountain as it passes through the vegetation zones. According to Nash et al (1991)[76], the playa has the highest soil moisture content (approximately  $0.27\text{cm}^3\text{cm}^{-3}$ ) as compared to the other zones. The soil moisture decreases as one moves up along the transect from the playa. The amount of soil water in the upper piedmont slope is the least with the amount of soil water averaging to about  $0.06\text{cm}^3\text{cm}^{-3}$ . The playa also possesses the highest water holding capacity with respect to the other zones because it has the highest mean clay content. Even though the upper piedmont slope records an average rainfall that is slightly higher than the other vegetations, the runoff water does have a tendency of converging in the playa because of its lower altitude as compared to the other zones.

#### 4.2.3 Data Used

Soil water contents were measured using the neutron probe in the area of interest– the Jornada control transect, which has ninety one stations. These soil water measurements have been collected since 1982. Station markers were installed with access tubes by them at 30 m intervals along the transect (Nash et al, 1991)[76] [7]. The data was collected once in a month. There are eighty nine neutron probe tubes found in the Jornada control transect which spans the vegetation zones. The table below displays the allocation of the transect stations and the corresponding vegetation zones that they pass through (Nash et al, 1991)[76].



No.	Name	Zones	Stations	
			Range	No.
1	Playa-grassland ( <i>Panicum obtusum</i> )		1-7	7
2	Playa fringe -shrubland ( <i>Prosopis glandulosa</i> )		8-10	3
3	Basin slope-grassland ( <i>Aristida longiseta</i> )		11-57	47
4	Bajada slopes- Shrubland ( <i>Larrea tridentata</i> )		58-72	15
5	Lower piedmont slope-grassland ( <i>Erioneuron pulchellum</i> )		73-81	9
6	Upper piedmont slope-grassland ( <i>Bouteloua eriopoda</i> )		82-89	8
7	Rocky slope-shrubland ( <i>Ericamera laricifolia</i> )		90 -91	2

Table 4.1: Vegetation Zones and Stations along the Jornada long term ecological research (JRN LTER) Control Transect

The soil moisture content measurements were collected at five different depths ( 30 cm, 60 cm, 90 cm, 110 cm and 130 cm ) at each of the access tubes in the control transect. The total depth of soil layer being observed for this study is 145 cm which is segmented into 5 layers. The soil moisture content measurement for each depth is taken within the bounds of the representative layers. The table below shows the different measurement depths and the corresponding thickness of the representative layer thickness.

Depth (cm)	Layer (cm)
30	45
60	30
90	25
110	20
130	25

Table 4.2: Depths of Measurement and Representative Layer Thickness

#### 4.2.4 Analysis of the Pixels

In this project, thirteen pixels, that are representative of most of the major vegetations in the area of interest, were studied. Each pixel was a square with dimension  $250m \times 250m$ .

The pixels are numbered from 0 to 12 in accordance with the indexing system used by python. The vegetations found on pixels 0, 1 and 2 are generally playa grasses with rings of mesquite. Pixels 3 through 9 are generally filled with

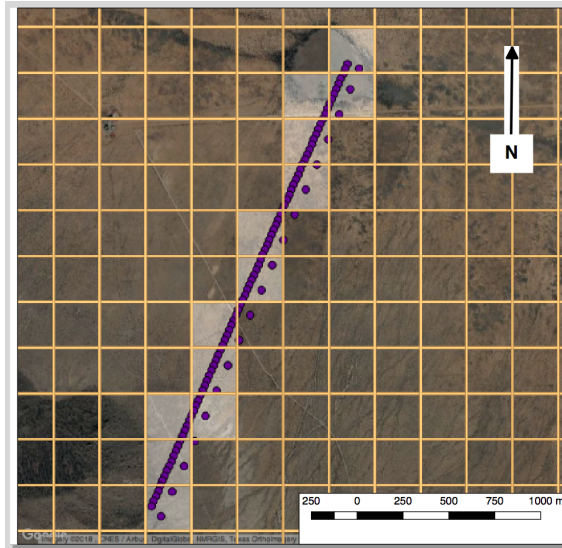


Figure 4.2: Locations of the 13 pixels along the Jornada Transect with Neutron Probe Tubes (Source: G. Parrish, Personal Communication, May 08, 2018)

mixed shrubs and grasses and pixels 10 to 12 are mostly Black Grama grasslands with some shrubs.

Pixel	Number of Access Tubes	Access Tube Numbers
0	2	C01–C02
1	2	C10–C11
2	7	C03–C09
3	10	C12–C21
4	8	C22–C29
5	9	C31–C39
6	9	C40–C48
7	7	C51–C57
8	9	C58–C66
9	5	C71–C75
10	4	C67–C70
11	9	C76–C84
12	5	C85–C89

Table 4.3: Pixels and Access tubes

The table above (table 4.3) shows the pixels used and the number of access tubes located on each of them. From the table, it can be seen that the pixels used only makes use of 86 of the access tubes because the other tubes are outside the range of the pixels. Access tubes C30, C49 and C50 are not used in the study.

## CHAPTER 5

### RESULTS AND DISCUSSIONS

#### 5.1 Introduction

This chapter essentially presents and analyzes the results obtained from using the history matching method to estimate the best fitting TAW values from modeled root zone soil moisture from the ETRM and observations of root zone soil from the neutron probe and remote sensing.

#### 5.2 ETRM Run

The ETRM Model was ran for all 13 pixels for a 14-year simulation period (January 1, 2000 to December 31, 2013) with a daily timestep. The model was ran for different TAW values, ranging from 25 mm to 600 mm at an interval of 25 mm. Also, for each pixel, the ETRM was ran at smaller intervals around the best fitting TAW values to refine the grid search and help smooth the chi square plots and produce more accurate estimates of TAW.

#### 5.3 Results and Discussions Using the Neutron Probe Data

##### 5.3.1 Estimating TAW Using the Neutron Probe Data

For all thirteen pixels, there are field root zone water fraction (RZWF) data from 1982 to 2015. However, only the values from the year 2000 and newer are used because of the time constraint of the ETRM. Using the history matching process, the best fitting (optimal) TAW (i.e. the TAW that yields the minimum chi square value) estimated for each pixel and the 95% region for the optimal TAW, as discussed in section 3.6.1, are tabulated in table 5.1 below:

Pixel	Optimal TAW (mm)	95% Confidence Interval
0	45	[33.51, 84.34]
1	50	[46.71, 77.00]
2	55	[41.90, 89.20]
3	55	[44.10, 88.40]
4	50	[47.80, 74.20]
5	60	[45.13, 85.58]
6	45	[41.86, 76.84]
7	150	[108.8, 216.8]
8	125	[72.00, 170.0]
9	75	[66.30, 143.7]
10	150	[112.2, 226.3]
11	75	[67.60, 153.2]
12	125	[77.70, 197.0]

Table 5.1: A Table of Optimal Total Available Water (TAW) and 95% Confidence Interval for all 13 Pixels Using Neutron Probe

The plots below show the trend of the chi square values as the TAW increases for each pixel. It also shows the TAW at which the minimum chi square value occurs and the 95% confidence region.

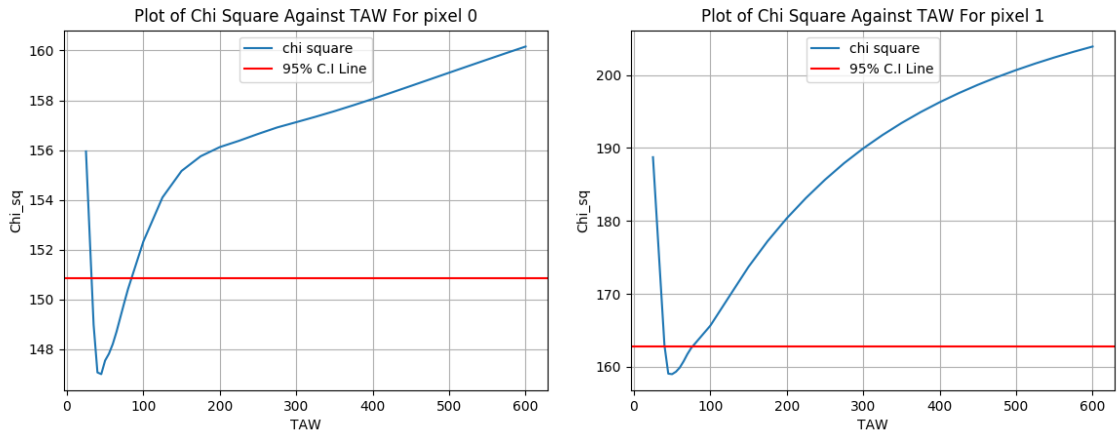


Figure 5.1: Chi Square Plots For all Thirteen Pixels (Pixels 0 and 1)

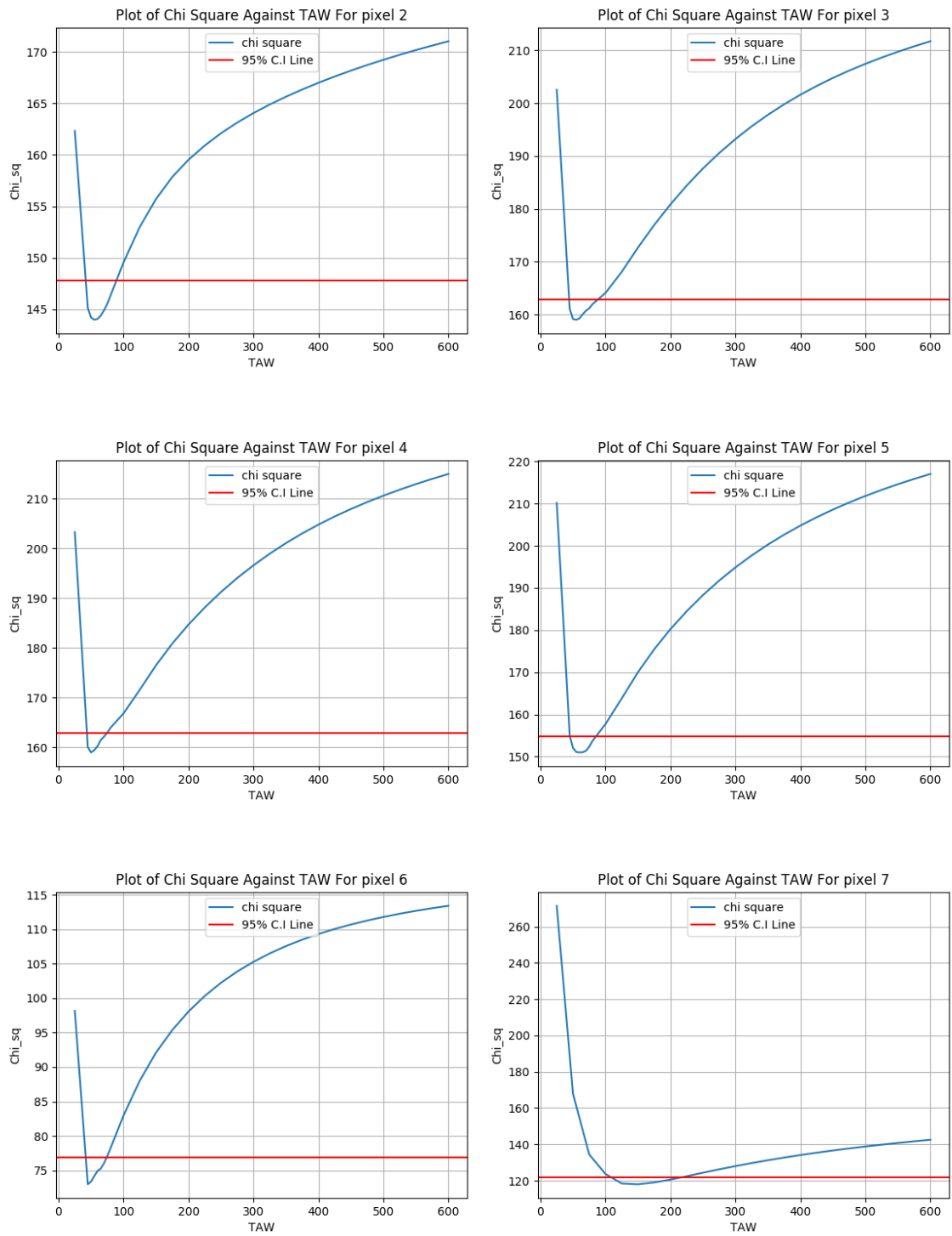


Figure 5.2: Chi Square Plots For all Thirteen Pixels (Pixels 2 – 7)

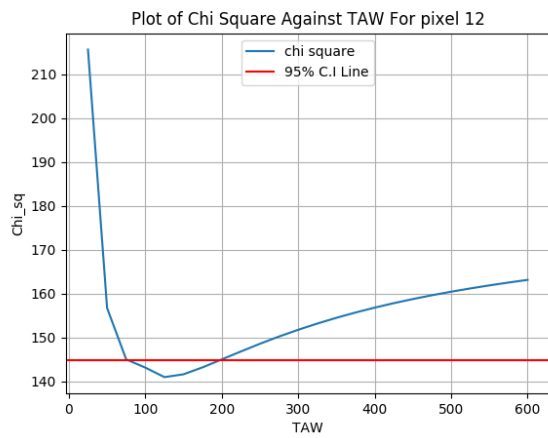
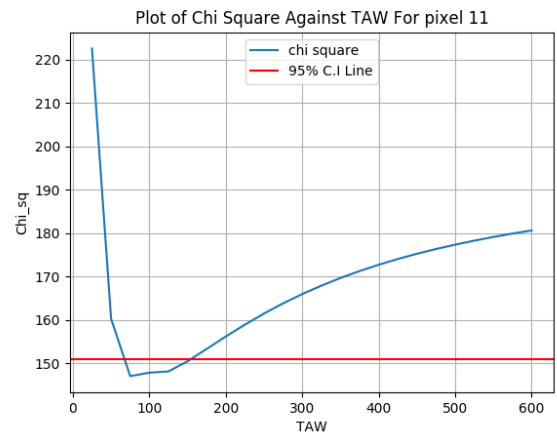
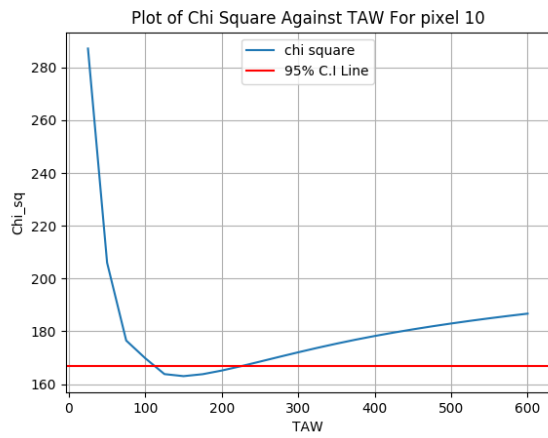
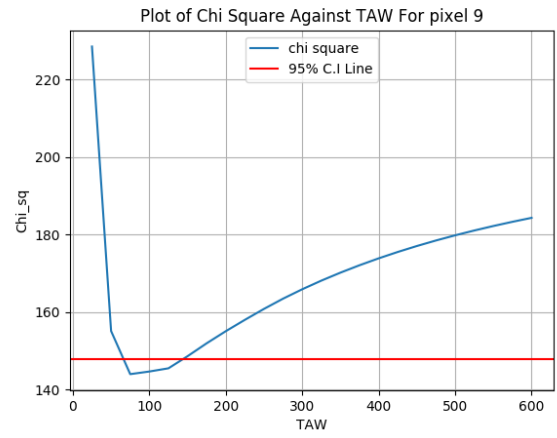
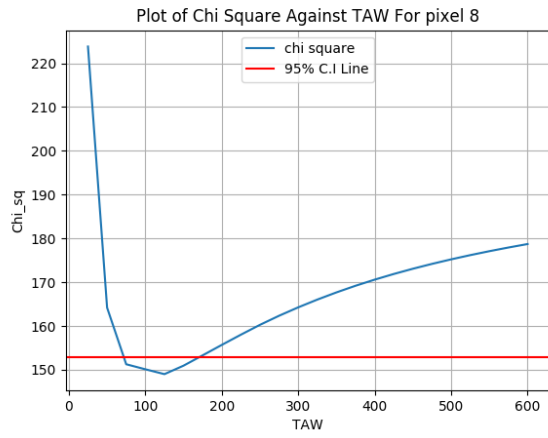


Figure 5.3: Chi Square Plots For all Thirteen Pixels (Pixels 8 – 13)

The table 5.2 below compares the best fitting TAW values to TAW values, estimated from soil maps, originally used in the ETRM.

<b>History Matched</b>			<b>Estimated From Soil Maps</b>	
Pixel	TAW (mm)	$\chi^2$ Value	TAW (mm)	$\chi^2$ Value
0	45	147.0	257	156.73
1	50	159.0	244	185.15
2	55	144.0	249	162.05
3	55	159.0	220	183.75
4	50	159.0	198	184.33
5	60	151.0	163	172.87
6	45	73.0	163	93.83
7	150	118.0	163	118.40
8	125	149.0	147	150.70
9	75	144.0	157	149.57
10	150	163.0	113	166.20
11	75	147.0	144	149.83
12	125	141.0	144	141.37

Table 5.2: Pixels and Corresponding Total Available Water (TAW) values Originally used in the Evapotranspiration and Recharge Model (ETRM)

From table 5.1 and table 5.2 above, it can be observed that the optimal TAW estimated using the history matching is notably different from the values originally used in the ETRM in pixels 0 to 6 and pixel 9. In these pixels, the history matched TAWs are consistently and significantly smaller than the ETRM values of TAW. The chi square values estimated by the history matching method are smaller as compared to the chi square values produced by the ETRM values of the TAW. This means that in these pixels, the history matched TAWs (and all the TAWs within the 95% confidence region) are better TAW values to use in the ETRM to produce better estimates of root zone soil moisture, ET and recharge than the values previously used.

In pixels 7 and 8, and pixels 10 to 12, the originally used TAW values are reasonably close to the history matched TAWs (i.e. the originally used TAW values lie within the 95% confidence region of the history matched TAW). This shows that the ETRM values of TAW fit the history reasonably well in these pixels.



### 5.3.2 Outliers

In order to determine if there are any days with very large residual outliers, the Z-score for each observation (day) was calculated and plotted as histograms. The Z-score is basically the measure of the number of standard deviations by which a given data point lies from its mean. For example, a Z-score of 0 indicates that the data component is equivalent to the mean, when the Z-score is +1, it indicates that the data component is one standard deviation greater than the mean and when Z-score is  $-3$ , it indicates that the data component is two standard deviations smaller than the mean.

For a particular day, if  $|Z| \geq 3$  (*i.e.*  $Z \geq 3$  or  $Z \leq -3$ ), that day is considered to be an outlier based on the empirical rule that 99.7% of the observations fall within three standard deviations of the mean. The Z-score is calculated for each day using:

$$Z = \frac{RZWF - RZSM_{(bestTAW)}}{s} \quad (5.1)$$

The plots below show the histograms of the Z-Score and the possible outliers:

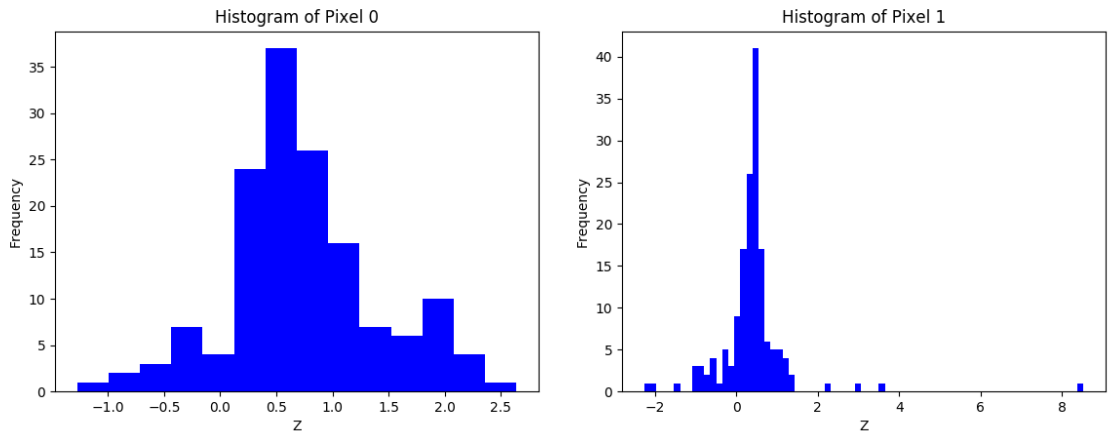


Figure 5.4: The Z-Score Histograms For all Thirteen Pixels (Pixels 0 and 1)

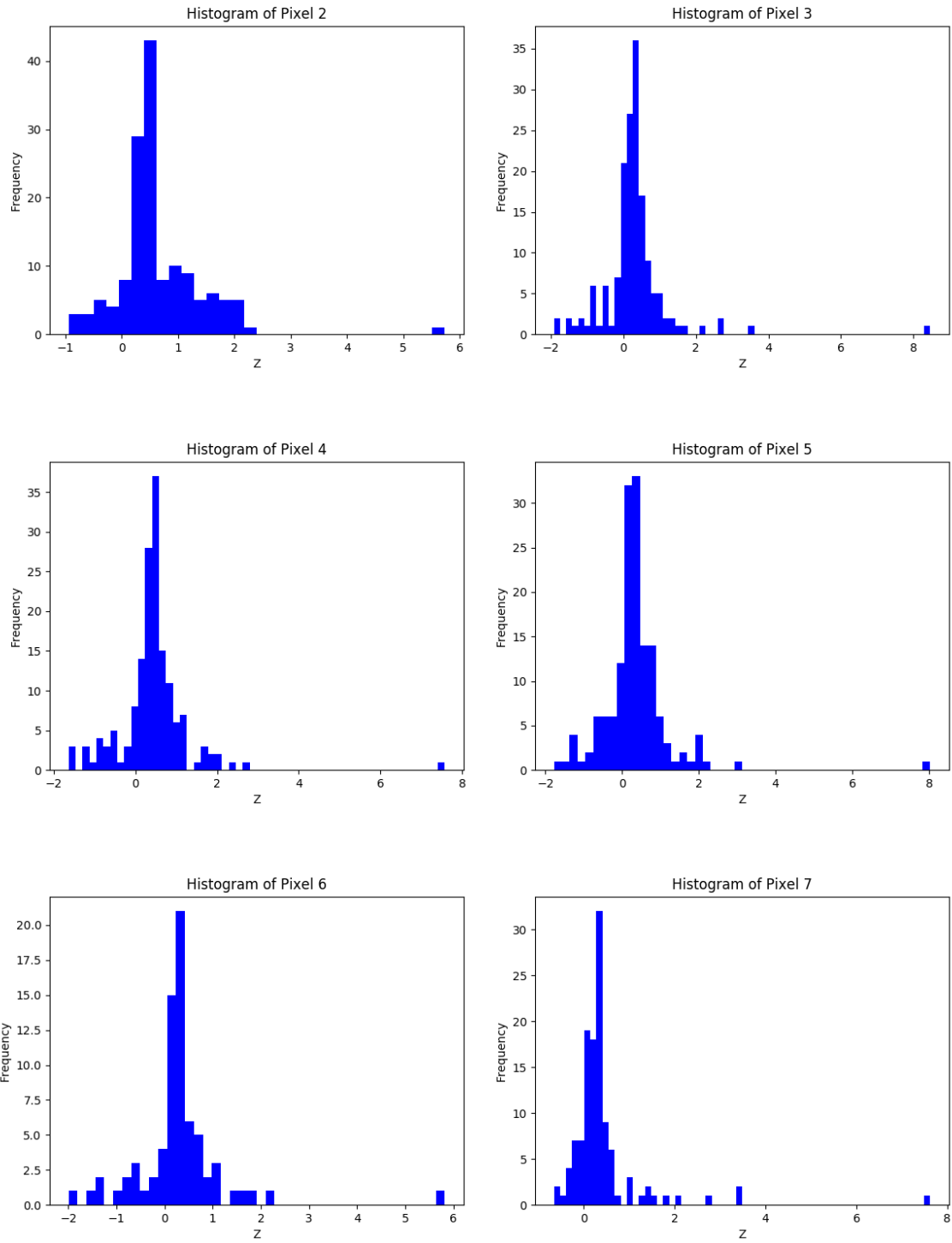


Figure 5.5: The Z-Score Histograms For all Thirteen Pixels (Pixels 2 – 7)

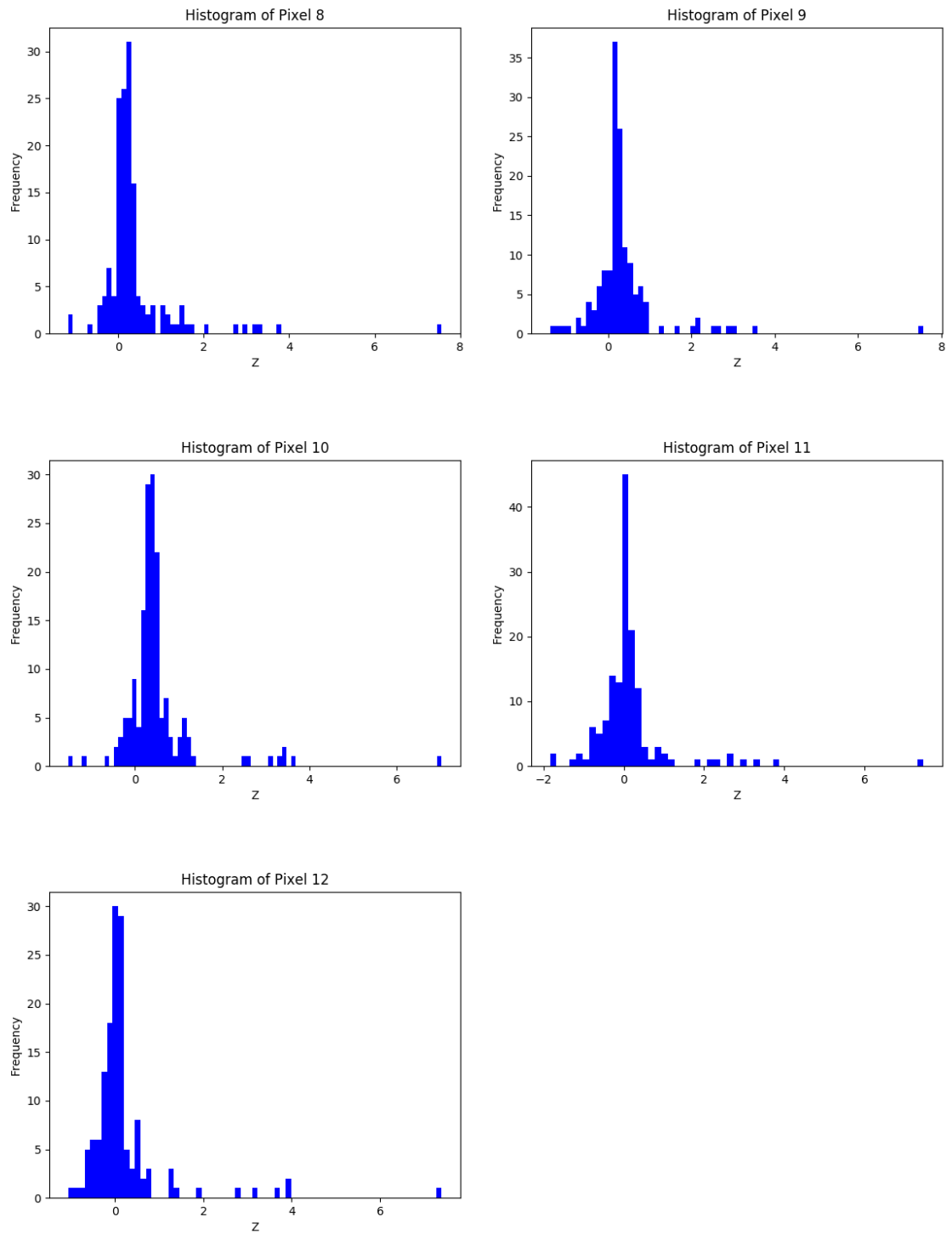


Figure 5.6: The Z-Score Histograms For all Thirteen Pixels (Pixel 8 – 12)

Based on the Z-scores calculated in equation (5.1) and the histograms above, the outliers and the dates on which they occurred are tabulated in the table below:

Pixel	Z	Dates(MM/DD/YYYY)
1	8.53	08/05/2011
	3.56	06/07/2010
2	5.68	08/05/2011
3	8.33	08/05/2011
	3.46	06/07/2010
4	7.58	08/05/2011
5	7.74	08/05/2011
6	5.92	08/05/2011
7	7.62	08/05/2011
	3.40	06/07/2010
	3.38	04/01/2010
8	7.58	08/05/2011
	3.73	06/07/2010
	3.36	04/01/2010
	3.24	07/30/2010
9	7.57	08/05/2011
	3.58	06/07/2010
	3.02	01/08/2010
10	7.02	08/05/2011
	3.62	06/07/2010
	3.44	07/07/2010
	3.42	04/01/2010
	3.32	07/30/2010
	3.14	01/08/2010
11	7.48	08/05/2011
	3.77	06/07/2010
	3.31	07/07/2010
12	7.40	08/05/2011
	3.98	04/01/2010
	3.89	01/08/2010
	3.61	07/07/2010
	3.17	08/07/2009

Table 5.3: Table of Outliers and Corresponding Dates

The table 5.3 indicates that observations on August 05, 2011 produces a big outlier that is consistent throughout almost all the pixels. On this day, even though the precipitation recorded is 0.51 mm, the precipitation recorded on the previous day is 16 mm. It is highly likely that the precipitation from the previous day had not fully evaporated or infiltrated the soil as at the time the soil moisture measurements were taken. This fits reasonably well with the assertion that the RZSM is significantly under predicted by the ETRM as compared to the soil moisture content measured using the neutron probe.

Another date that appeared in 7 out of the 13 pixels as an outlier is June 07, 2010. This day, however, recorded 0.51 mm as the precipitation. The field site recorded zero precipitation for about six weeks prior to June 07, 2010 . This does not agree with this date being a positive outlier. This could be as a result of some variations and limitations of the ETRM.

### 5.3.3 Estimating TAW Using the Remote Sensing Data

For all thirteen pixels, root zone water fraction (RZWF) values were calculated from remote sensing observations using equation (3.15). Using the history matching process, the best fitting (optimal) TAW (i.e. the TAW that occurs at the minimum chi square value) estimated for each pixel , as discussed in section 3.6.1, are tabulated in table 5.4 below:

Pixel	Optimal TAW (mm)
0	50
1	50
2	275
3	25
4	25
5	25
6	25
7	25
8	25
9	25
10	25
11	25
12	25

Table 5.4: A Table of the best fitting Total Available Water (TAW) for all 13 Pixels Using Remote Sensing

The plots below shows the trend of the chi square values as the TAW increases for each pixel. It also shows the TAW at which the minimum chi square value occurs and the 95% confidence region.

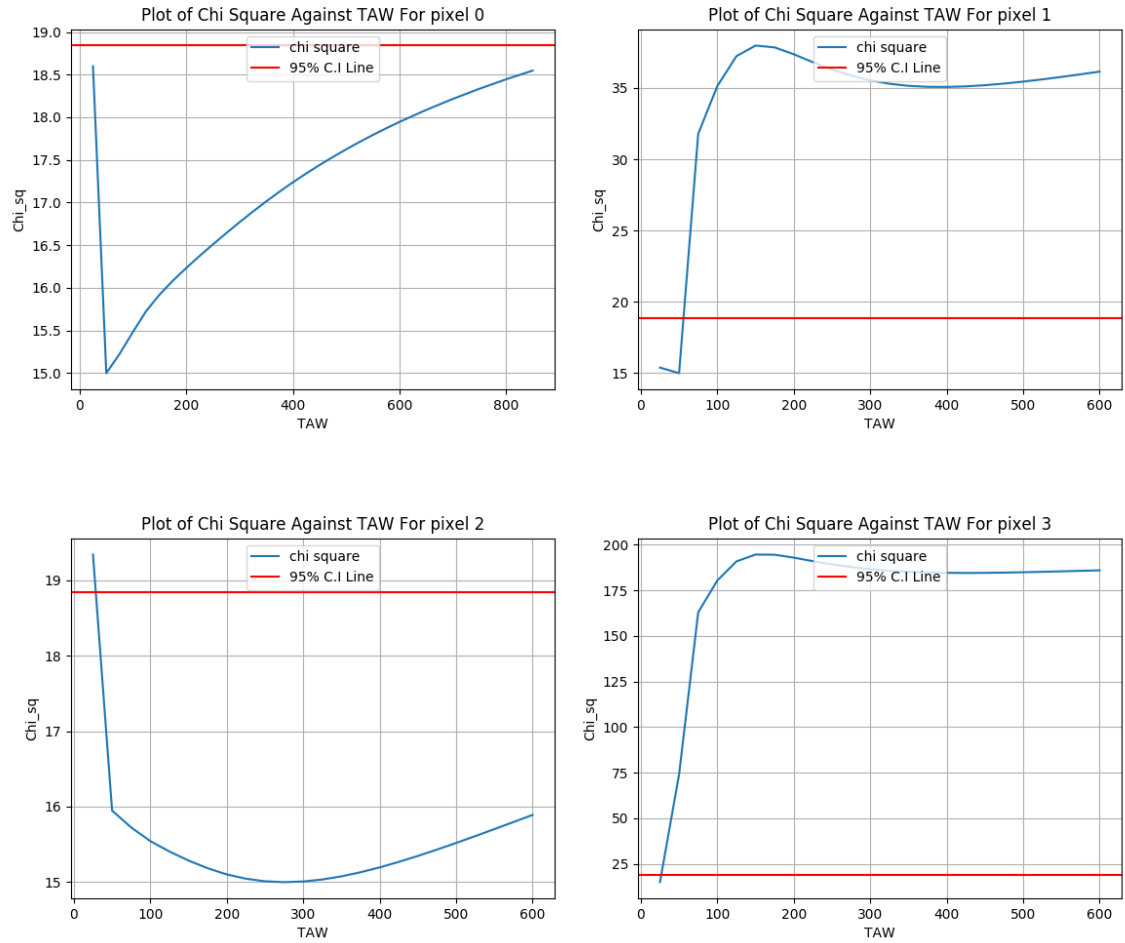


Figure 5.7: Remote Sensing: Chi Square Plots For all Thirteen Pixels (Pixels 0 – 3)

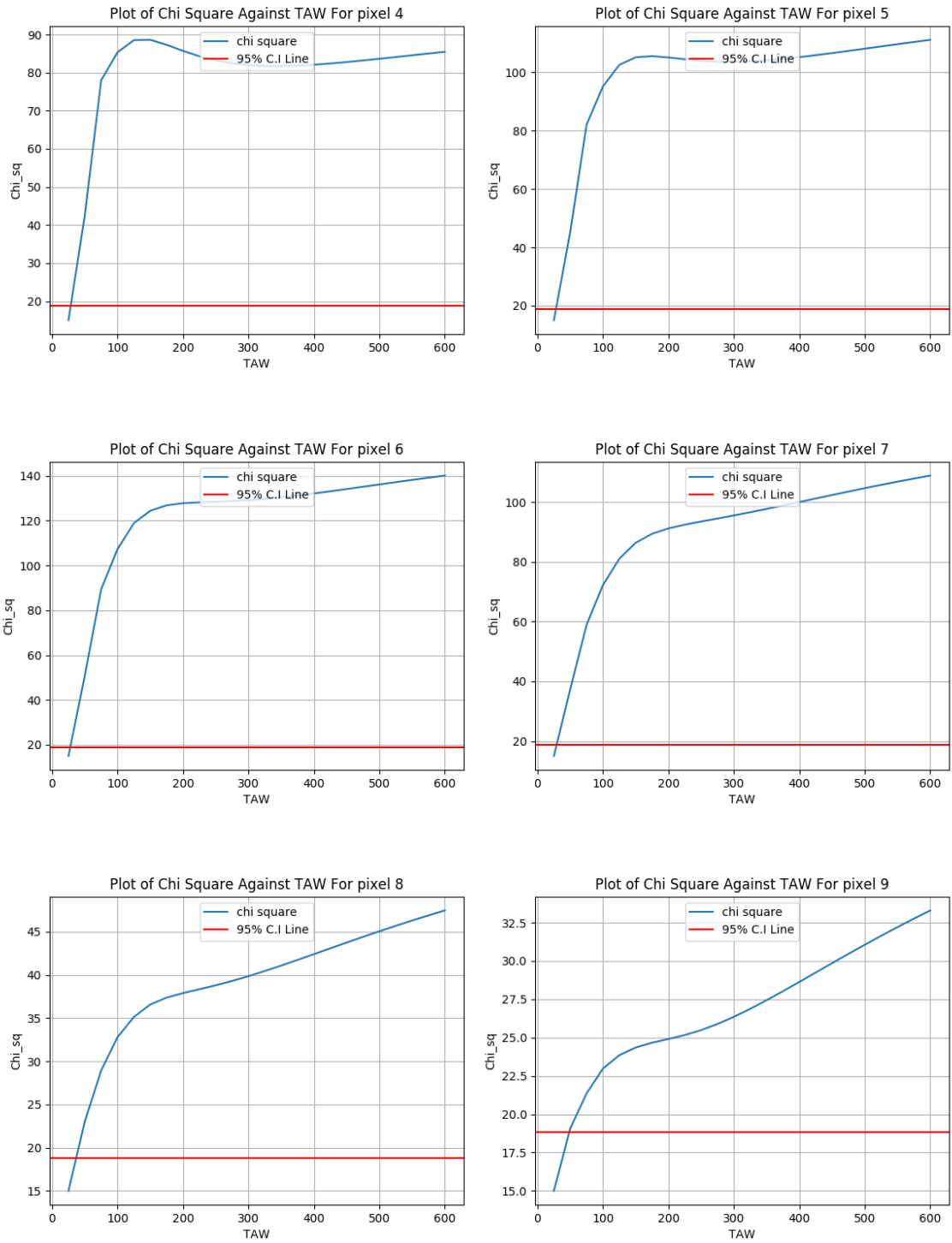


Figure 5.8: Remote Sensing: Chi Square Plots For all Thirteen Pixels (Pixels 4 – 9)

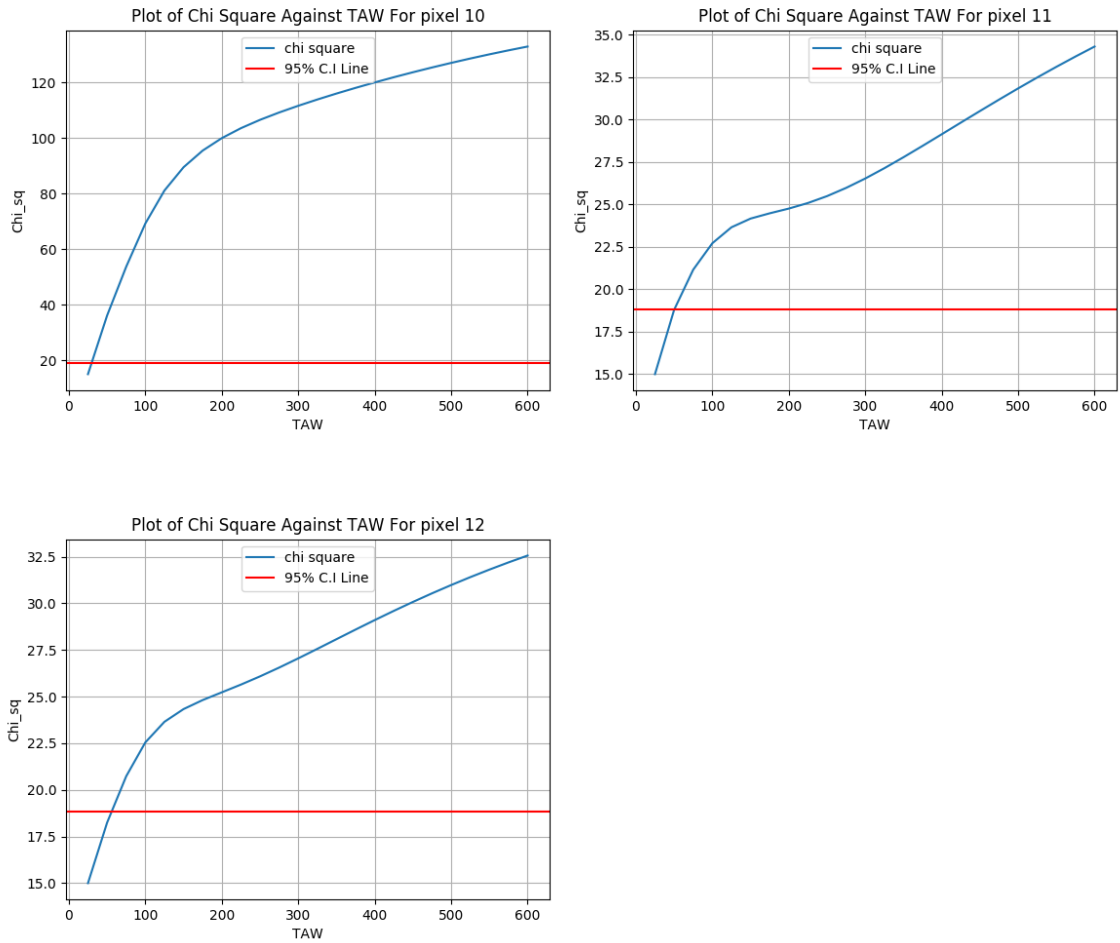


Figure 5.9: Remote Sensing: Chi Square Plots For all Thirteen Pixels (Pixels 10 – 13)

From the table plots above, it can be seen that in most of the pixels, the plots produced are not distinctive enough to show typical TAWs at which the minimum chi square occurs. It can also be seen that there is no precision to the estimates (i.e. a 95% confidence region cannot be obtained precisely for the TAW estimates from the remote sensing data). This shows that the results produced by the History matching for the remote sensing data are not reliable and therefore, are not useful. This could be because:

- i. There was not enough data to develop a definitive pattern of the soil moisture over the historical period. All the thirteen pixels had remote sensing observations for only 16 days.



- ii. The data used was not extensive. For almost all the pixels, the remote sensing data recorded 0s (which represent dates when no soil moisture was recorded). This makes the data unreliable to use.

### 5.3.4 Comparing the Root Zone Moisture Content of the Neutron Probe and Remote Sensing

So as to ascertain whether the root zone soil moisture from the neutron probe and remote sensing are comparable, the RZWF values from both methods are shown in the table 5.5 below. Since the data are not collected on the same day, the comparison is done with days that are close enough to each other (at most 5 days difference).

Remote Sensing			Neutron Probe	
Pixel	RZWF	Date	RZWF	Date
0	0.00	06/05/2001	0.161	06/04/2001
	0.00	05/07/2002	0.323	05/10/2002
	0.00	06/08/2008	0.138	06/06/2008
1	0.00	06/05/2001	0.119	06/04/2001
	0.00	05/07/2002	0.106	05/10/2002
	0.00	06/08/2008	0.118	06/06/2008
	0.00	04/30/2011	0.182	04/25/2011
2	0.006	06/05/2001	0.133	06/04/2001
	0.00	05/07/2002	0.196	05/10/2002
	0.00	06/08/2008	0.081	06/06/2008
	0.00	04/30/2011	0.118	04/25/2011
3	0.00	06/05/2001	0.079	06/04/2001
	0.00	05/07/2002	0.083	05/10/2002
	0.00	06/08/2008	0.072	06/06/2008
4	0.00	06/05/2001	0.097	06/04/2001
	0.00	05/07/2002	0.105	05/10/2002
	0.00	06/08/2008	0.102	06/06/2008
	0.00	04/30/2011	0.127	04/25/2011
5	0.00	06/05/2001	0.064	06/04/2001
	0.00	05/07/2002	0.075	05/10/2002
	0.00	06/08/2008	0.062	06/06/2008
6	0.00	05/07/2002	0.089	05/10/2002
	0.00	04/25/2011	0.097	04/25/2011

7	0.00	06/05/2001	0.056	06/04/2001
	0.00	05/07/2002	0.057	05/10/2002
	0.00	06/05/2008	0.05	06/05/2008
8	0.00	06/05/2001	0.062	06/05/2001
	0.00	05/07/2002	0.052	05/10/2002
	0.00	06/08/2008	0.049	06/05/2008
	0.00	04/30/2011	0.097	04/26/2011
9	0.00	06/05/2001	0.039	06/05/2001
	0.00	05/07/2002	0.038	05/10/2002
	0.00	06/08/2008	0.037	06/05/2008
	0.00	04/30/2011	0.092	04/26/2011
10	0.00	06/05/2001	0.103	06/05/2001
	0.00	05/07/2002	0.091	05/10/2002
	0.00	06/08/2008	0.094	06/05/2008
	0.00	04/30/2011	0.146	04/26/2011
11	0.00	06/05/2001	0.028	06/05/2001
	0.00	05/07/2002	0.016	05/10/2002
	0.00	06/08/2008	0.010	06/05/2008
	0.00	04/30/2011	0.084	04/26/2011
12	0.00	06/05/2001	0.02	06/05/2001
	0.00	05/07/2002	0.017	05/10/2002
	0.089	06/08/2008	0.018	06/05/2008
	0.00	04/30/2011	0.069	04/26/2011

Table 5.5: Comparing Root Zone Water Fraction (RZWF) Values of Neutron Probe and Remote Sensing

From the table, it can be deduced that the RZWF from the neutron probe are consistently higher than the RZWF from remote sensing.

#### 5.4 Sensitivity Analysis of the Annual Average Recharge Estimate to the TAW

To analyze the sensitivity of the annual recharge to TAW, the ETRM was used to estimate the recharge using the best fitting TAW values from both the neutron probe and remotely-sensed observations and the TAW values, estimated from soil maps, originally used in the ETRM . The results are tabulated in table 5.6 below

Pixel	Neutron Probe Recharge (mm/yr)	Remote Sensing Recharge (mm/yr)	Original TAW Recharge (mm/yr)
0	7.9	6.3	0
1	7.5	7.5	0
2	1.2	0	0
3	6.4	27.1	0
4	7.4	26.3	0
5	4.5	25.3	0
6	7.1	24.6	0
7	0	24.2	0
8	0	23.8	0
9	3.8	23.4	0
10	0	25.3	0.6
11	4.0	23.5	0
12	0	23.7	0

Table 5.6: Comparing the Annual Average Recharge Rates Between the Estimated and Original Values of the Total Available Water

From the table 5.6 above, it can be seen that the ETRM with the new TAW parameters produced recharge estimates that are significantly higher than zero in most the pixels. When the original TAW values were used, the ETRM estimated the recharge to be zero or close to zero in all the pixels.

McKenna and Sala, 2018 [71] estimated that the annual average recharge estimate in the Jornada playa was 6 mm per year. Using the TAWs estimated from the neutron probe observations, the average of the annual recharge estimates in pixels 0, 1 and 2 (i.e. the pixels found in the playa) is 5.5 mm per year. The portion of the playa covered by the three pixels is very small when compared to the playas in the Jornada . Due to this, comparing the average annual estimates of the three pixels and the playa would be quite unrealistic. However, in terms of magnitude, it can be deduced that the average annual recharge estimate is quite reasonable. Also, Shomaker and Finch, 1996 [101], estimated the average annual mountain-front recharge in the Jornada Basin to be 4.13 mm per year. Also, the average of the annual recharge for all thirteen pixels, is 3.81 mm per year. This estimate is reasonable in terms of magnitude even though it covers only a small fraction of the Jornada basin. Looking at the average annual recharge estimated from the ETRM (when the TAWs estimated from the remotely-sensed soil moisture observations are used), it shows that the average recharge is highly overestimated in most of the pixels. The table also shows that the recharge estimate is underestimated in the ETRM when the original TAWs are used in the model.

## CHAPTER 6

### CONCLUSIONS AND RECOMMENDATIONS

#### 6.1 Conclusion

Using the history matching method, the TAW was optimized by using root zone soil moisture values from the ETRM and observations of root zone soil water content from field measurements. From the results and the findings of this study, the following conclusions were drawn:

- (i) The Total Available Water (TAW) parameter has an effect on the estimates of root zone soil moisture.
- (ii) The best fitted TAW values estimated from the history matching method were consistently smaller than the TAW values originally used in the ETRM. The chi square reports showed that using the best fitting TAW values (or any TAW value within the 95% confidence region) to run the model produced better RZSM results (i.e. their RZSM values from the model was considerably close to the field measurements). The smaller TAW values produced by the history matching could be due to the following reasons:
  - a. Run-on water was not modeled in the ETRM. This affects the historical RZSM values modeled by the ETRM in the playa pixels because most of the run off water from the upslope surroundings and vegetations run across the surfaces into the playa because its nature (low-lying and basin-like). This causes the playa to be consistently flooded with the run on water. This is reflected on the field measurements of the root zone soil moisture content but not on the ETRM-modeled RZSM.
  - b. Most of the pixels are covered with sparse vegetation which leads to partial coverage of the pixel by the root zone. This has effects on the TAW values because the vegetation (land) cover maps produce the estimates of the rooting depth used in the calculation of the TAW. The sparsity of vegetation cover on the pixels leads to inaccurate rooting depth, leading to an overestimation of the TAW.

- (iii) From the results, the maximum amount of plant-available water that can be held within the root zone of the soil was smaller for the pixels 0 through 6 and generally increased as one moves up across the transect. This is because, as one moves across the the transect from pixel 0 to pixel 12, there is a change in vegetation i.e. the vegetation (mostly grassland and shrubs) becomes denser as one moves up the transect. This causes a rise in the estimate of the rooting depth, leading to an increment in the TAW.
- (iv) The best fitting TAWs estimated from this study seem to be smaller than what was expected for the area studied according to expert opinion (Fred Phillips, Personal Communication, August 01, 2018). This could be due to the following reasons: (i) The thickness of the soil layer considered in this study was 1.45 m. However, in practice, the soil layer could be as thick as 20 m. TAWs estimated at this thickness will most likely be higher than the ones produced with the 1.45 m layer thickness. (ii) The TAWs produced are spatially averaged over a particular pixel. In the Jornada, there are spots where the soil is bare and there are no activities (plant growth, transpiration) going on there. This could cause the spatial average of the TAW to be smaller than specific estimates of the TAW in the pixel.
- (v) The history matching method, as developed in this study, worked very well with extensive data (like in the case of the neutron probe data) but did not produce any reliable results with limited data (like in the case of the remote sensing).
- (vi) The remote sensing data did not work because the data was not extensive and the data was collected on days with no moisture recorded. The history matching method might work with remotely-sensed observations of the root zone water content if more of the remote sensing data are collected on days or a few days after a wetting event has occurred.
- (vii) The groundwater recharge estimate produced by the ETRM is highly sensitive to the choice of TAW value used in the model. The TAW values estimated from the history matching method, using the neutron probe observations, produced reasonable estimates of the groundwater recharge in terms of magnitude. The study also showed that the average rate of recharge is generally higher in the playa as compared to the whole of the Jornada.

Also, the the annual average recharge estimates were mostly overestimated when the TAW estimates produced from the remotely-sensed observations were used in the ETRM. The estimates were also seen to be underestimated when the original TAW values were used in the ETRM.

It can be concluded that smaller TAW values generally indicates an increase in the recharge. This is because smaller TAW means smaller storage in the

soil, which means there will be excess water that cannot be stored in the root zone. This also increases the quantity of water that could infiltrate the soil thereby, increasing the recharge.

## 6.2 Limitations

The ETRM can only produce results for a simulation period starting from the year 2000 because some of the input parameters used in the ETRM were not available until the year 2000.

Also, the history matching method of determining the root zone soil moisture content cannot yet be scaled to the entire state until comprehensive remote sensing RZWF that are comparable to the neutron probe are collected and used.

Another limitation is that the ETRM model takes a considerable amount of time to run ( i.e. for one TAW, it takes about 4 hours to run the ETRM for a particular pixel for the historical period observed, 2000 to 2013) and takes up a lot of storage memory. The model can also not run for specific dates; It is built to run for all days in the year selected. This outputs a lot of redundant data especially when only a few days of the year are needed for an analysis.

Also, the best fitting TAW values were estimated by doing a grid search based on the intervals of TAW values that was run. This is time-consuming and produces less accurate results by limiting the value of the best fitting TAW to the values of TAW used to run the model. Also, it might become infeasible to use the grid search method when working with very large data and millions of pixels. An optimization method (such as the Levenberg-Marquardt method) could be used to produce more accurate results. However, the model would have to be rewritten to support this.

Additionally, it is assumed in this study that the root zone soil moisture is found in the first two meters of the soil. This may be true for areas where plants have shallow roots but this assumption does not hold for many zones in the Jornada where some shrubs have extensive roots that are more than two meters deep in the soil. This causes the total available water to be highly underestimated in those areas since the history matching method is unable to account for the water outside the depth worked with.

## 6.3 Recommendations

Based on the results, conclusions and limitations discussed, the following recommendations have been made to be applied to get more accurate results for the statewide water assessment:

- (i) The ETRM can be modified to run one pixel at a time and adjust the TAW by writing a subroutine, which would estimate the best TAW to use, into the model. It can also be modified to reduce the time and memory it consumes.
- (ii) Obtain more remotely sensed soil moisture observations and apply the history matching method to estimate the TAWs. Compare these TAW values to the ones estimated from for the neutron probe soil moisture observations.
- (iii) Modify the method to estimate the best fitting TAW for the pixels in the entire state of New Mexico.

## APPENDIX A

### ADDITIONAL INFORMATION ON THE ACCESS TUBES

#### A.1 Minimum and Maximum Storages For Each Access Tube (cm)

C01:	(20.0, 60.0)	C31:	(7.0, 33.0)	C62:	(2.0, 26.0)
C02:	(20.0, 56.0)	C32:	(8.0, 34.0)	C63:	(3.0, 28.0)
C03:	(20.0, 61.0)	C33:	(5.0, 28.0)	C64:	(3.0, 28.0)
C04:	(20.0, 63.0)	C34:	(6.0, 31.0)	C65:	(6.0, 30.0)
C05:	(17.0, 62.0)	C35:	(5.0, 31.0)	C66:	(4.0, 28.0)
C06:	(19.0, 54.0)	C36:	(6.0, 32.0)	C67:	(4.0, 31.0)
C07:	(14.0, 44.0)	C37:	(7.0, 30.0)	C68:	(3.0, 30.0)
C08:	(10.0, 41.0)	C38:	(7.0, 32.0)	C69:	(3.0, 28.0)
C09:	(12.0, 36.0)	C39:	(6.0, 31.0)	C70:	(5.0, 32.0)
C10:	(09.0, 31.0)	C40:	(7.0, 32.0)	C71:	(4.0, 31.0)
C11:	(08.0, 32.0)	C41:	(5.0, 31.0)	C72:	(5.0, 30.0)
C12:	(05.0, 27.0)	C42:	(5.0, 31.0)	C73:	(2.0, 29.0)
C13:	(03.0, 28.0)	C43:	(6.0, 33.0)	C74:	(1.0, 27.0)
C14:	(04.0, 30.0)	C44:	(4.0, 28.0)	C75:	(1.0, 27.0)
C15:	(04.0, 29.0)	C45:	(5.0, 30.0)	C76:	(0.0, 25.0)
C16:	(04.0, 30.0)	C46:	(4.0, 31.0)	C77:	(0.0, 26.0)
C17:	(05.0, 30.0)	C47:	(6.0, 30.0)	C78:	(0.0, 25.0)
C18:	(04.0, 30.0)	C48:	(5.0, 30.0)	C79:	(0.0, 26.0)
C19:	(05.0, 33.0)	C51:	(4.0, 29.0)	C80:	(0.0, 25.0)
C20:	(06.0, 32.0)	C52:	(4.0, 28.0)	C81:	(0.0, 21.0)
C21:	(06.0, 33.0)	C53:	(5.0, 30.0)	C82:	(0.0, 25.0)
C22:	(08.0, 35.0)	C54:	(5.0, 30.0)	C83:	(1.0, 26.0)
C23:	(07.0, 33.0)	C55:	(4.0, 29.0)	C84:	(1.0, 27.0)
C24:	(07.0, 34.0)	C56:	(40.0, 29.0)	C85:	(0.0, 26.0)
C25:	(08.0, 36.0)	C57:	(3.0, 30.0)	C86:	(0.0, 23.0)
C26:	(10.0, 35.0)	C58:	(3.0, 24.0)	C87:	(1.0, 25.0)
C27:	(09.0, 32.0)	C59:	(2.0, 28.0)	C88:	(1.0, 24.0)
C28:	(08.0, 35.0)	C60:	(1.0, 27.0)	C89:	(0.0, 23.0)
C29:	(08.0, 32.0)	C61:	(2.0, 27.0)		



## APPENDIX B

### PYTHON CODES

#### B.1 General Python script Used to Find the Best Fitting TAW

```
import sys
import numpy as np
import matplotlib.pyplot as plt
from matplotlib.pyplot import *
import pandas as pd
from scipy import special, optimize
from scipy.stats import chi2
import os
import math

def sse_calc(path):
df = pd.read_csv(path)

# Finding the residuals
dat = []
for i in range(len(df.index)):
x = df['mean_rzswf'][i] - df['rzsm'][i]

dat.append(x)

df['E'] = pd.Series(dat)

#Finding the Residual Sum of Squares

df['r'] = df['E']
df['chi'] = df['r']**2

u = pd.unique(df['taw'])

sum = []
```

```

num=[]

for i in range(len(u)):
    y = 0
    n=0
    for j in range(len(df.index)):
        if df['taw'][j] == u[i]:
            y = y + df['chi'][j]
            n=n+1
    sum.append(y)
    num.append(n)

plot = pd.DataFrame([])
plot['chi_sq'] = pd.Series(sum)
plot ['dof'] = pd.Series(num)
plot['taw'] = u

return plot

def chi2_calc(main_path):
    out_files = []
    for a, b, c in os.walk(main_path, topdown=True):

        for file in c:
            if file.endswith('.csv'):
                fullpath = os.path.join(a, file)
                out_files.append(fullpath)

    print "out", out_files

    dict = {}
    for path in out_files:
        #print path
        #print "path len {}".format(len(path))
        name_lst = path.split("/")
        name = name_lst[-1]
        #print "name", name
        name = name[:-4]
        #print "name update", name
        c = sse_calc(path)
        dict["{}".format(name)] = c

```

```

for key, val in dict.iteritems():

x = val['taw']
y = val['chi_sq']

df = val['dof']- 1
nu = df ** (0.5)
norm = val['chi_sq'] ** (0.5)
s      = norm / nu

min = y[0]
for a in y:
    if a < min:
        min = a
print "smallest", min

for i in range(len(y)):
    if y[i]==min:
        minT=x[i]

print "Min TAW", minT

smin = (min ** (0.5))/ (df[0]**(0.5))
sq = smin ** 2
chimin = min/sq
c = chimin + 3.841459
t = y/sq

print "s at min TAW", smin
print "nu", df[0]
print "bound", c
print "var for min",sq
print "min chi", min
print "chi2 min", chimin
print '''====='''
plt.plot(x, t, label='chi square')

plt.title("Plot of Chi Square Against TAW For {}".format(key))

plt.xlabel('TAW')
plt.ylabel('Chi_sq')

```

```

plt.grid(True)

plt.axhline(y= c, color='r', linestyle='-', label = '95% C.I Line')
plt.legend(loc='upper center')

fig1 = plt.gcf()
plt.show()
plt.draw()
#fig1.savefig("plot" + str(i) + ".png", dpi=100)
fig1.savefig("{}".format(key) + ".png", dpi=100)

def run():
main_path = "/Users/new/Desktop/new"
#main_path = "/Users/new/Desktop/noise 0.0005"

#plot_graph(main_path)

chi2_calc(main_path)

#plot_graph(dict)

if __name__ == "__main__":

print "Calculating chi square"

# call master function

run()

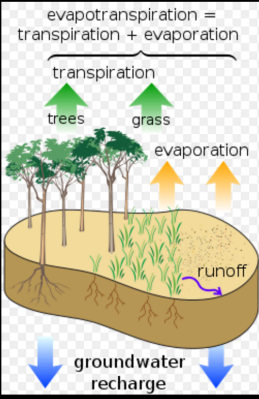
```

## APPENDIX C

## PERMISSIONS


The Hydrological Cycle (Figure 1.1) by [M. W. Toews](#) is licensed under [CC BY 4.0](#)

← → ↻ [https://en.wikipedia.org/wiki/Evapotranspiration#/media/File:Surface\\_water\\_cycle.svg](https://en.wikipedia.org/wiki/Evapotranspiration#/media/File:Surface_water_cycle.svg) ☆ 🔴






The diagram illustrates the water cycle at the Earth's surface. At the top, it states:  $\text{evapotranspiration} = \text{transpiration} + \text{evaporation}$ . Below this, a bracket groups 'transpiration' and 'evaporation'. 'transpiration' is shown with green arrows pointing up from 'trees' and 'grass'. 'evaporation' is shown with orange arrows pointing up from the soil surface. A purple arrow labeled 'runoff' flows to the right on the ground surface. At the bottom, blue arrows labeled 'groundwater recharge' point downwards into the ground.

Water cycle of the Earth's surface, showing the individual components of transpiration and evaporation that make up evapotranspiration. Other closely related processes shown are [runoff](#) and [groundwater recharge](#). [More details](#)

 [M. W. Toews](#) - Own work

Conceptual diagram of near-surface hydrology, showing [evapotranspiration](#), [evaporation](#), [transpiration](#), [runoff](#), and [recharge](#) processes.

 [CC BY 4.0](#)  
 File: Surface water cycle.svg  
 Created: 1 October 2007

The Map of The Jornada LTER Station (Figure 4.1) was downloaded and edited from the [LTER Site Profiles](#) and it is permitted to be reused under a [Creative Commons BY-SA 4.0 license](#).<sup>1</sup>

The screenshot displays the LTER Network website interface. At the top, the logo for the National Science Foundation LTER Network is visible, along with navigation menus for 'THE NETWORK', 'SITES', 'RESEARCH', 'EDUCATION', 'USING LTER SCIENCE', and 'NEWS'. A search icon is also present.

The main content area features a map of the Jornada Basin LTER station, highlighted in yellow. The map includes labels for various locations such as Pinos Altos, Silver City, Bayard, Hillsboro, Arrey, Hatch, Las Cruces, White Sands, and Huelmoan AFB. A red pin marks the location of the Jornada Basin LTER station. Below the map, a list of other LTER sites is provided, including Andrews Forest LTER (AND), Arctic LTER (ARC), Baltimore Ecosystem Study (BES), Beaufort Lagoon Ecosystem LTER (BLE), Bonanza Creek LTER (BNZ), California Current Ecosystem LTER (CCE), Cedar Creek Ecosystem Science Reserve (CDR), Central Arizona – Phoenix LTER (CAP), Coweeta LTER (CWT), Florida Coastal Everglades LTER (FCE), Georgia Coastal Ecosystems LTER (GCE), Harvard Forest LTER (HFR), Hubbard Brook LTER (HBR), Jornada Basin LTER (JRN), Kellogg Biological Station LTER (KBS), Konza Prairie LTER (KNZ), LTER Network (NWK), LTER Network Communications Office (NCO), Luquillo LTER (LUQ), McMurdo Dry Valleys LTER (MCM), Mo'orea Coral Reef LTER (MCR), Niwot Ridge LTER (NWT), North Temperate Lakes LTER (NTL), Northeast U.S. Shelf (NES), Northern Gulf of Alaska (NGA), Palmer Antarctica LTER (PAL), Plum Island Ecosystems LTER (PIE), Santa Barbara Coastal LTER (SBC), Sevilleta LTER (SEV), and Virginia Coast Reserve LTER (VCR).

To the right of the map, there are four small images showing the landscape and research activities at the station. Below these images, there are links for 'Site Profile >' and 'Jornada Basin LTER Homepage >'. At the bottom of the page, there is a green footer section containing navigation links for 'Events', 'Document Archive', 'People', 'Publications', 'Opportunities', and 'Contact Us'. It also includes copyright information: '© 2018 LTER. Managed by LTER Network Communications Office, NCEAS, UCSB, 735 State Street, Suite 300, Santa Barbara, CA 93101. Except where otherwise noted, material may be re-used under a Creative Commons BY-SA 4.0 license.' and a disclaimer: 'This material is based upon work supported by the National Science Foundation under grant DEB#1545288, 10/1/2015-9/30/19. Any opinions, findings, conclusions, or recommendations expressed in the material are those of the author(s) and do not necessarily reflect the views of the National Science Foundation.'

<sup>1</sup>Texts in blue are links to the web pages containing the image and license

## REFERENCES

- [1] Creosote bush. [mojavedesert.net/plants/shrubs/creosote.html](http://mojavedesert.net/plants/shrubs/creosote.html). Accessed: 2018-07-30.
- [2] Evapotranspiration - the water cycle. <https://water.usgs.gov/edu/watercycleevapotranspiration.html>. Accessed: 2018-06-30.
- [3] *Flourensia cernua*. <https://www.fs.fed.us/database/feis/plants/shrub/flocer/all.html>. Accessed: 2018-07-06.
- [4] History matching. [http://www.glossary.oilfield.slb.com/Terms/h/history\\_matching.aspx](http://www.glossary.oilfield.slb.com/Terms/h/history_matching.aspx) . Accessed: 2018-07-09.
- [5] Honey mesquite. [http://calscape.org/Prosopis-glandulosa-\(\)](http://calscape.org/Prosopis-glandulosa-()). Accessed: 2018-07-30.
- [6] The hydrologic cycle. [https://www.nwrfc.noaa.gov/info/water\\_cycle/hydrology.cgi](https://www.nwrfc.noaa.gov/info/water_cycle/hydrology.cgi). Accessed: 2018-06-30.
- [7] Jornada basin LTER. <https://lternet.edu/site/jornada-basin-lter>. Accessed: 2018-07-03.
- [8] Jornada LTER site description. <https://jornada.nmsu.edu/lter>. Accessed: 2018-05-22.
- [9] Limitations of MODIS data. <https://nsidc.org/support/21553418-What-are-the-limitations-of-MODIS-data->. Accessed: 2018-07-02.
- [10] LTER Site Profiles. <https://lternet.edu/site/?m=JRN>. Accessed: 2018-05-28.
- [11] MODIS components. <https://modis.gsfc.nasa.gov/about/components.php>. Accessed: 2018-04-28.
- [12] Neutron moisture meters. [ucmanagedrought.ucdavis.edu/PDF/DROUGHT\\_WEB\\_NEUTRON\\_PRB.pdf](http://ucmanagedrought.ucdavis.edu/PDF/DROUGHT_WEB_NEUTRON_PRB.pdf) . Accessed: 2018-07-29.
- [13] Neutron moisture meters. <https://sanangelo.tamu.edu/extension/agronomy/agronomy-publications/grain-sorghum-production-in-west-central-texas/how-to-estimate-soil-moisture-by-feel/soil-moisture-measuring-devices/neutron-moisture-meters>. Accessed: 2018-07-03.
- [14] New Mexico Water Resource Research Institute. <https://nmwrri.nmsu.edu>. Accessed: 2018-04-17.

- [15] Soil data viewer. [https://www.nrcs.usda.gov/wps/portal/nrcs/detailfull/soils/survey/geo/?cid=nrcs142p2\\_053620](https://www.nrcs.usda.gov/wps/portal/nrcs/detailfull/soils/survey/geo/?cid=nrcs142p2_053620). Accessed: 2018-07-01.
- [16] Soil moisture water balance models. <https://www.ncdc.noaa.gov/monitoring-references/dyk/soil-moisture-models>. Accessed: 2018-07-03.
- [17] Statewide water assessment. <https://nmwrri.nmsu.edu/category-blocks-swa/#DSWB>. Accessed: 2018-04-17.
- [18] A summary of the hydrological cycle. [http://ww2010.atmos.uiuc.edu/\(Gh\)/guides/mtr/hyd/smry.rxml](http://ww2010.atmos.uiuc.edu/(Gh)/guides/mtr/hyd/smry.rxml). Accessed: 2018-06-30.
- [19] The USGS land cover. <https://landcover.usgs.gov/usgslandcover.php>. Accessed: 2018-06-19.
- [20] Web soil survey. <https://websoilsurvey.sc.egov.usda.gov/App/WebSoilSurvey.aspx>. Accessed: 2018-06-19.
- [21] Why use eddy covariance to measure flux? [https://www.licor.com/env/applications/eddy\\_covariance](https://www.licor.com/env/applications/eddy_covariance). Accessed: 2018-07-02.
- [22] Alfieri, L., Claps, P., D’Odorico, P., Laio, F., and Over, T. M. (2008). An analysis of the soil moisture feedback on convective and stratiform precipitation. *Journal of Hydrometeorology*, 9(2):280–291.
- [23] Allen, R., Irmak, A., Trezza, R., Hendrickx, J. M., Bastiaanssen, W., and Kjaersgaard, J. (2011). Satellite-based et estimation in agriculture using SEBAL and METRIC. *Hydrological Processes*, 25(26):4011–4027.
- [24] Allen, R. G. (2011). Skin layer evaporation to account for small precipitation events-an enhancement to the FAO-56 evaporation model. *Agricultural Water Management*, 99(1):8–18.
- [25] Allen, R. G., Pereira, L. S., Raes, D., and Smith, M. (1998a). FAO irrigation and drainage paper no. 56. *Rome: Food and Agriculture Organization of the United Nations*, 56(97):e156.
- [26] Allen, R. G., Pereira, L. S., Raes, D., Smith, M., et al. (1998b). Crop evapotranspiration-guidelines for computing crop water requirements-FAO irrigation and drainage paper 56. *FAO, Rome*, 300(9):D05109.
- [27] Allen, R. G., Pereira, L. S., Smith, M., Raes, D., and Wright, J. L. (2005). FAO-56 dual crop coefficient method for estimating evaporation from soil and application extensions. *Journal of irrigation and drainage engineering*, 131(1):2–13.
- [28] Allen, R. G., Tasumi, M., Morse, A., Trezza, R., Wright, J. L., Bastiaanssen, W., Kramber, W., Lorite, I., and Robison, C. W. (2007a). Satellite-based energy balance for mapping evapotranspiration with internalized calibration (METRIC)- applications. *Journal of irrigation and drainage engineering*, 133(4):395–406.



- [29] Allen, R. G., Tasumi, M., and Trezza, R. (2007b). Satellite-based energy balance for mapping evapotranspiration with internalized calibration (METRIC)-model. *Journal of irrigation and drainage engineering*, 133(4):380–394.
- [30] Anderson, M. C., Norman, J. M., Mecikalski, J. R., Otkin, J. A., and Kustas, W. P. (2007). A climatological study of evapotranspiration and moisture stress across the continental United States based on thermal remote sensing: 1. model formulation. *Journal of Geophysical Research: Atmospheres*, 112(D10).
- [31] Aster, R. C., Borchers, B., and Thurber, C. H. (2011). *Parameter estimation and inverse problems*, volume 90. Academic Press.
- [32] Bacchi, O., Reichardt, K., and Calvache, M. (2002). Neutron and gamma probes: Their use in agronomy. *Training course series... Vienna: International Atomic Energy Agency*, page 75.
- [33] Bastiaanssen, W., Pelgrum, H., Droogers, P., De Bruin, H., and Menenti, M. (1997). Area-average estimates of evaporation, wetness indicators and top soil moisture during two golden days in efeda. *Agricultural and Forest Meteorology*, 87(2-3):119–137.
- [34] Bastiaanssen, W. G., Menenti, M., Feddes, R., and Holtslag, A. (1998a). A remote sensing surface energy balance algorithm for land (SEBAL): 1. formulation. *Journal of hydrology*, 212:198–212.
- [35] Bastiaanssen, W. G., Pelgrum, H., Wang, J., Ma, Y., Moreno, J., Roerink, G., and Van der Wal, T. (1998b). A remote sensing surface energy balance algorithm for land (SEBAL): Part 2: Validation. *Journal of hydrology*, 212:213–229.
- [36] Bastiaanssen, W. G. M. (1995). *Regionalization of surface flux densities and moisture indicators in composite terrain: A remote sensing approach under clear skies in Mediterranean climates*. SC-DLO.
- [37] Belmans, C., Wesseling, J., and Feddes, R. A. (1983). Simulation model of the water balance of a cropped soil: SWATRE. *Journal of hydrology*, 63(3-4):271–286.
- [38] Bolle, H.-J., Andre, J.-C., Arrue, J., Barth, H., Bessemoulin, P., Brasa, A., De Bruin, H., Cruces, J., Dugdale, G., Engman, E., et al. (1993). EFEDA: European field experiment in a desertification-threatened area. In *Annales Geophysicae*, volume 11, pages 173–189. Copernicus.
- [39] Burk, L. and Dalgliesh, N. (2008). Estimating plant available water capacity—a methodology. *Canberra: CSIRO Sustainable Ecosystems*, page 40.
- [40] Cassel, D. and Nielsen, D. (1986). Field capacity and available water capacity. *Methods of Soil Analysis: Part 1-Physical and Mineralogical Methods*, (methodsofsoilan1):901–926.

- [41] Center, C. P. et al. (2004). Climate prediction center (cpc) global monthly leaky bucket soil moisture analysis.
- [42] Cosgrove, B. A., Lohmann, D., Mitchell, K. E., Houser, P. R., Wood, E. F., Schaake, J. C., Robock, A., Marshall, C., Sheffield, J., Duan, Q., et al. (2003). Real-time and retrospective forcing in the north american land data assimilation system (NLDAS) project. *Journal of Geophysical Research: Atmospheres*, 108(D22).
- [43] Daly, C., Neilson, R. P., and Phillips, D. L. (1994). A statistical-topographic model for mapping climatological precipitation over mountainous terrain. *Journal of applied meteorology*, 33(2):140–158.
- [44] Davies, J. and Allen, C. (1973). Equilibrium, potential and actual evaporation from cropped surfaces in southern ontario. *Journal of Applied Meteorology*, 12(4):649–657.
- [45] De Bruin, H. (1983). A model for the Priestley-Taylor parameter  $\alpha$ . *Journal of climate and applied meteorology*, 22(4):572–578.
- [46] Dumedah, G., Walker, J. P., and Merlin, O. (2015). Root-zone soil moisture estimation from assimilation of downscaled soil moisture and ocean salinity data. *Advances in Water Resources*, 84:14–22.
- [47] Duncan, J., Stow, D., Franklin, J., and Hope, A. (1993). Assessing the relationship between spectral vegetation indices and shrub cover in the jornada basin, New Mexico. *International Journal of Remote Sensing*, 14(18):3395–3416.
- [48] Engman, E. T. and Chauhan, N. (1995). Status of microwave soil moisture measurements with remote sensing. *Remote Sensing of Environment*, 51(1):189–198.
- [49] Evett, S. (2008). Neutron moisture meters. Technical report.
- [50] Fleming, K., Hendrickx, J. M., and Hong, S.-h. (2005). Regional mapping of root zone soil moisture using optical satellite imagery. In *Targets and Backgrounds XI: Characterization and Representation*, volume 5811, pages 159–171. International Society for Optics and Photonics.
- [51] Foolad, F., Blankenau, P., Kilic, A., Allen, R. G., Huntington, J. L., Erickson, T. A., Ozturk, D., Morton, C. G., Ortega, S., Ratcliffe, I., et al. (2018). Comparison of the automatically calibrated google evapotranspiration application-EEFlux and the manually calibrated METRIC application.
- [52] Ford, T., Harris, E., and Quiring, S. (2014). Estimating root zone soil moisture using near-surface observations from SMOS. *Hydrology and Earth System Sciences*, 18(1):139.
- [53] Garner, R. E. (2002). Plant fact sheet- black grama. [https://www.nrcs.usda.gov/Internet/FSE\\_PLANTMATERIALS/.../azpmcfs5602.pdf](https://www.nrcs.usda.gov/Internet/FSE_PLANTMATERIALS/.../azpmcfs5602.pdf). Accessed: 2018-05-23.

- [54] Goslee, S., Havstad, K., Peters, D., Rango, A., and Schlesinger, W. (2003). High-resolution images reveal rate and pattern of shrub encroachment over six decades in New Mexico, USA. *Journal of Arid Environments*, 54(4):755–767.
- [55] Greenland, D. and Anderson, J. (2018). Jornada basin site description. <https://lternet.edu/site/jornada-basin-lter/>. Accessed: 2018-07-03.
- [56] Hassan-Esfahani, L., Torres-Rua, A., and McKee, M. (2015). Assessment of optimal irrigation water allocation for pressurized irrigation system using water balance approach, learning machines, and remotely sensed data. *Agricultural Water Management*, 153:42–50.
- [57] Havstad, K. M., Huenneke, L. F., and Schlesinger, W. H. (2006). *Structure and function of a Chihuahuan desert ecosystem: the Jornada Basin long-term ecological research site*. Oxford University Press.
- [58] Hendrickx, J. M., Allen, R. G., Brower, A., Byrd, A. R., Hong, S.-h., Ogden, F. L., Pradhan, N. R., Robison, C. W., Toll, D., Trezza, R., et al. (2016). Benchmarking optical/thermal satellite imagery for estimating evapotranspiration and soil moisture in decision support tools. *JAWRA Journal of the American Water Resources Association*, 52(1):89–119.
- [59] Hendrickx, J, M. H. and Cadol, D. (2015). New Mexico statewide water assessment: Soil water balance method for statewide evapotranspiration assessment - year two. preprint on webpage at <https://nmwrri.nmsu.edu/wp-content/SWWA/Reports/Hendrickx/December2015/Report.pdf>.
- [60] Hendrickx, J, M. H., Schmutge, H., and Cadol, D. (2015). Improving evapotranspiration estimation using remote sensing technology. preprint on webpage at <https://nmwrri.nmsu.edu/wp-content/SWWA/Reports/Hendrickx/April%202015/report.pdf>.
- [61] Huang, J., van den Dool, H. M., and Georgarakos, K. P. (1996). Analysis of model-calculated soil moisture over the United States (1931–1993) and applications to long-range temperature forecasts. *Journal of Climate*, 9(6):1350–1362.
- [62] Israelsen, O. W. and West, F. L. R. (1922). *Water-holding capacity of irrigated soils*. Number 183. Utah Agricultural College Experiment Station.
- [63] Jensen, M. E. and Allen, R. G. (2016). *Evaporation, evapotranspiration, and irrigation water requirements*. American Society of Civil Engineers.
- [64] Ketchum, D. (2016). High-resolution estimation of groundwater recharge for the entire state of New Mexico using a soil- water-balance model. Master’s thesis, New Mexico Tech, Socorro, NM.

- [65] Ketchum, D., Newton, B. T., and Phillips, H. F. (2015). Statewide water assessment: Recharge data compilation and recharge area identification for the state of New Mexico.
- [66] Kirkham, M. B. (2014). *Principles of soil and plant water relations*. Academic Press.
- [67] Kornelsen, K. C. and Coulibaly, P. (2014). Root-zone soil moisture estimation using data-driven methods. *Water Resources Research*, 50(4):2946–2962.
- [68] Ladson, A., Lander, J., Western, A., Grayson, R., and Zhang, L. (2006). Estimating extractable soil moisture content for australian soils from field measurements. *Soil Research*, 44(5):531–541.
- [69] Lewis, C. S., Geli, H. M., and Neale, C. M. (2014). Comparison of the nldas weather forcing model to agrometeorological measurements in the western united states. *Journal of hydrology*, 510:385–392.
- [70] MacMahon, J. A. and Wagner, F. H. (1985). Mojave, sonoran and chihuahuan deserts of north america. *Ecosystems of the world*.
- [71] McKenna, O. P. and Sala, O. E. (2018). Groundwater recharge in desert playas: current rates and future effects of climate change. *Environmental Research Letters*, 13(1):014025.
- [72] Mecikalski, J. R., Diak, G. R., Anderson, M. C., and Norman, J. M. (1999). Estimating fluxes on continental scales using remotely sensed data in an atmospheric-land exchange model. *Journal of applied meteorology*, 38(9):1352–1369.
- [73] Milly, P. (1994). Climate, soil water storage, and the average annual water balance. *Water Resources Research*, 30(7):2143–2156.
- [74] Nash, M., Daugherty, L., Wierenga, P., Nance, S., and Gutjahr, A. (1988). Horizontal and vertical kriging of soil properties along a transect in southern New Mexico. *Soil Science Society of America Journal*, 52(4):1086–1090.
- [75] Nash, M. H. H. (1985). *Numerical classification spatial dependence, and vertical kriging of soil sites in southern New Mexico*. PhD thesis, New Mexico State University.
- [76] Nash, M. S., Wierenga, P. J., and Gutjahr, A. (1991). Time series analysis of soil moisture and rainfall along a line transect in arid rangeland. *Soil Science*, 152(3):189–198.
- [77] Newton, T., Phillips, F., and Rhinehart, A. (2016). New Mexico statewide water assessment: Recharge quantification and recharge model assessment for the state of New Mexico. preprint on webpage at <https://nmwrri.nmsu.edu/wp-content/SWWA/Reports/Newton/January2016/Report.pdf>.

- [78] Nie, W., Yuan, Y., Kepner, W., Erickson, C., and Jackson, M. (2012). Hydrological impacts of mesquite encroachment in the upper San Pedro watershed. *Journal of Arid Environments*, 82:147–155.
- [79] Pelgrum, H. and Bastiaanssen, W. (1996). An intercomparison of techniques to determine the area-averaged latent heat flux from individual in situ observations: A remote sensing approach using the european field experiment in a desertification-threatened area data. *Water Resources Research*, 32(9):2775–2786.
- [80] Peters, D. P. and Gibbens, R. P. (2006). *Plant communities in the Jornada Basin: the dynamic landscape*. Oxford University Press: New York, NY, USA.
- [81] Peterson K., Roach J., T. B. (2015). A dynamic statewide water budget for New Mexico: Phase 1 - major river basins. New Mexico Water Resources Research Institute Draft Technical Completion Report Index # 124273. Las Cruces.
- [82] Priestley, C., Taylor, R., et al. (1972). On the assessment of surface heat flux and evaporation using large-scale parameters. *Monthly weather review*, 100(2):81–92.
- [83] Ratliff, L., Ritchie, J., and Cassel, D. (1983). Field-measured limits of soil water availability as related to laboratory-measured properties 1. *Soil Science Society of America Journal*, 47(4):770–775.
- [84] Rhinehart, A., Timmons, S., Felix, B., and Pokorny, C. (2015). Groundwater level and storage changes - regions of New Mexico. preprint on webpage at <https://nmwrri.nmsu.edu/wp-content/SWWA/Reports/Timmons/June%202015%20FINAL/report.pdf>.
- [85] Rhinehart, A., Timmons, S., Felix-Kludt, B., Pokorny, C., and Mamer, E. (2016). Groundwater level and storage changes in alluvial basins along the Rio Grande, New Mexico. preprint on webpage at <https://nmwrri.nmsu.edu/wp-content/SWWA/Reports/Timmons/January2016/Report.pdf>.
- [86] Ritchie, J. (1981a). Soil water availability. *Plant and soil*, 58(1-3):327–338.
- [87] Ritchie, J. T. (1981b). Water dynamics in the soil-plant-atmosphere system. *Plant and Soil*, 58(1-3):81–96.
- [88] Roach, J., Tidwell, V., Thompson, B., and Peterson, K. (2016). A dynamic statewide water budget for New Mexico. preprint on webpage at <https://nmwrri.nmsu.edu/wp-content/SWWA/Reports/Roach/January2016/Report.pdf>.
- [89] Romano, N. and Santini, A. (2002). Water retention and storage, in methods of soil analysis. part 1, edited by j. dane and c. topp. pages 721–738.
- [90] Samani, A. and Bawazir, S. (2015). Improving evapotranspiration estimation using remote sensing technology. *Technical Completion Report, Account Number (Index#)*, 125548.

- [91] Samani, A. and Bawazir, S. (2016). Improving evapotranspiration estimation using remote sensing technology. preprint on webpage at <https://nmwrrri.nmsu.edu/wp-content/SWWA/Reports/Bawazir/January2016/Report.pdf>.
- [92] Samani, Z., Bawazir, A. S., Skaggs, R. K., Bleiweiss, M. P., Piñon, A., and Tran, V. (2007). Water use by agricultural crops and riparian vegetation: an application of remote sensing technology. *Journal of Contemporary Water Research & Education*, 137(1):8–13.
- [93] Schaake, J. C., Duan, Q., Koren, V., Mitchell, K. E., Houser, P. R., Wood, E. F., Robock, A., Lettenmaier, D. P., Lohmann, D., Cosgrove, B., et al. (2004). An intercomparison of soil moisture fields in the north american land data assimilation system (nldas). *Journal of Geophysical Research: Atmospheres*, 109(D1).
- [94] Schmugge, T. (1998). Applications of passive microwave observations of surface soil moisture. *Journal of Hydrology*, 212:188–197.
- [95] Scott, C. A., Bastiaanssen, W. G., and Ahmad, M.-u.-D. (2003). Mapping root zone soil moisture using remotely sensed optical imagery. *Journal of Irrigation and Drainage Engineering*, 129(5):326–335.
- [96] Senay, G., Leake, S., Nagler, P., Artan, G., Dickinson, J., Cordova, J., and Glenn, E. (2011). Estimating basin scale evapotranspiration (ET) by water balance and remote sensing methods. *Hydrological Processes*, 25(26):4037–4049.
- [97] Senay, G. B. (2008). Modeling landscape evapotranspiration by integrating land surface phenology and a water balance algorithm. *Algorithms*, 1(2):52–68.
- [98] Senay, G. B., Bohms, S., Singh, R. K., Gowda, P. H., Velpuri, N. M., Alemu, H., and Verdin, J. P. (2013). Operational evapotranspiration mapping using remote sensing and weather datasets: A new parameterization for the sseb approach. *JAWRA Journal of the American Water Resources Association*, 49(3):577–591.
- [99] Senay, G. B., Budde, M., Verdin, J. P., and Melesse, A. M. (2007). A coupled remote sensing and simplified surface energy balance approach to estimate actual evapotranspiration from irrigated fields. *Sensors*, 7(6):979–1000.
- [100] Sesnie, S. E., Dickson, B. G., Rosenstock, S. S., and Rundall, J. M. (2012). A comparison of landsat tm and modis vegetation indices for estimating forage phenology in desert bighorn sheep (*ovis canadensis nelsoni*) habitat in the Sonoran desert, USA. *International Journal of Remote Sensing*, 33(1):276–286.
- [101] Shomaker, J. W. and Finch, S. T. (1996). *Multilayer Ground-water Flow Model of Southern Jornada Del Muerto Basin, Dona Ana County, New Mexico and Predicted Effects of Pumping Wells LRG-430-S29 And-S-30*. John Shomaker & Associates, Incorporated.

- [102] Singh, R. K., Senay, G. B., Velpuri, N. M., Bohms, S., Scott, R. L., and Verdin, J. P. (2013). Actual evapotranspiration (water use) assessment of the colorado river basin at the landsat resolution using the operational simplified surface energy balance model. *Remote Sensing*, 6(1):233–256.
- [103] Smith, E., Hsu, A., Crosson, W., Field, R., Fritschen, L., Gurney, R., Kanemasu, E., Kustas, W., Nie, D., Shuttleworth, W., et al. (1992). Area-averaged surface fluxes and their time-space variability over the FIFE experimental domain. *Journal of Geophysical Research: Atmospheres*, 97(D17):18599–18622.
- [104] Toews, M. W. Conceptual diagram of near-surface hydrology, showing evapotranspiration, evaporation, transpiration, runoff, and recharge processes. [https://en.wikipedia.org/wiki/Evapotranspiration#/media/File:Surface\\_water\\_cycle.svg](https://en.wikipedia.org/wiki/Evapotranspiration#/media/File:Surface_water_cycle.svg). Lincensed under CC BY 4.0; Accessed: 2018-06-17.
- [105] Wierenga, P. (1987). Variation of soil and vegetation with distance along a transect in the chihuahuan desert. *J Arid Environ*, 13:53–63.
- [106] Williams, D., Cable, W., Hultine, K., Hoedjes, J., Yopez, E., Simonneaux, V., Er-Raki, S., Boulet, G., De Bruin, H., Chehbouni, A., et al. (2004). Evapotranspiration components determined by stable isotope, sap flow and eddy covariance techniques. *Agricultural and Forest Meteorology*, 125(3-4):241–258.
- [107] Willman, S. E. and Carroll, K. C. (2015). *Assessment of Spatiotemporal Groundwater Level Changes Throughout New Mexico*. PhD thesis, New Mexico State University.
- [108] Xia, Y., Sheffield, J., Ek, M. B., Dong, J., Chaney, N., Wei, H., Meng, J., and Wood, E. F. (2014). Evaluation of multi-model simulated soil moisture in nldas-2. *Journal of hydrology*, 512:107–125.

Estimating The Total Available Water For The Prediction Of Root Zone Soil  
Moisture Using Evapotranspiration and Recharge Model

by

Juliet Ablah Ayertey

Permission to make digital or hard copies of all or part of this work for personal or classroom use is granted without fee provided that copies are not made or distributed for profit or commercial advantage and that copies bear this notice and the full citation on the last page. To copy otherwise, to republish, to post on servers or to redistribute to lists, requires prior specific permission and may require a fee.

